*Geophys. J. Int.* (2002) **148,** 1–33

# Palaeomagnetism of East Siberian traps and kimberlites: two new poles and palaeogeographic reconstructions at about 360 and 250 Ma

Vadim A. Kravchinsky,[1,2,3,*] Konstantin M. Konstantinov,[1] Vincent Courtillot,[3] Jams I. Savrasov,[4] Jean-Pierre Valet,[3] Sergey D. Cherniy,[4] Sergey G. Mishenin[5] and Boris S. Parasotka[4]

[1] *East-Siberian Research Institute of Geology, Geophysics and Mineral Resources, Ministry of Natural Resources, Irkutsk* 664007, *Russia*
[2] *Institute of Geochemistry, Siberian Branch of Russian Academy of Science, Irkutsk* 664033, *Russia*
[3] *Laboratoire de Paléomagnétisme, Institut de Physique du Globe de Paris,* 4 *place Jussieu,* 75252 *Paris Cedex* 05, *France*
[4] *Botuobinskaya Expedition, Diamonds Russia-Sakha Enterprise, Mirniy* 678170, *Russia*
[5] *Amakinskaya Expedition, Diamonds Russia-Sakha Enterprise, Aikhal* 678190, *Russia*

Accepted 2001 June 20. Received 2001 June 13; in original form 2000 December 12

## SUMMARY

We studied basalt sills and dykes and kimberlite pipes from the eastern part of the Siberian platform. These are spread out over a few hundred kilometres and are divided into two age groups: Late Permian–Early Triassic (Mir, Aikhal and Olenyek regions) and Late Devonian–Early Carboniferous (Viluy and Markha basins, Aikhal region). The palaeomagnetic poles determined for each sill or dyke are statistically different from each other, but averaging all corresponding directions from these sills and dykes with those from kimberlites of different generations yields results with acceptable statistics. This is probably due to the averaging out of secular variation and/or changes in magnetic polarity. The resulting palaeomagnetic poles allow one to reconstruct the palaeopositions of Siberia during the two large flood basalt events at about 360 and 250 Ma. A significant rotation of the Siberian platform during the Devonian and Carboniferous is suggested. The new data are in general agreement with some earlier palaeomagnetic poles for the Late Permian–Early Triassic traps of the Tungusska basin, and significantly reduce uncertainties for previous Late Devonian–Early Carboniferous Siberian poles, which were very scattered. Together with geological and absolute age data, the palaeomagnetic data support the hypothesis that kimberlite magmatism and trap intrusions were both rapid and relatively close in time. The 360 Ma event is emerging as a magmatic event with considerable extent over the Russian and Siberian platforms, related to incipient continental break-up and triple junction formation, possibly at or near the time of the Frasnian–Famennian mass extinction.

**Key words:** kimberlites, palaeomagnetism, palaeoreconstructions, rifting, Siberia, traps.

## INTRODUCTION

The kimberlites and Siberian trap formations have been studied palaeomagnetically in Siberia since 1963 (Savrasov & Kamisheva 1963; Davydov & Kravchinsky 1971; Kamysheva 1973; Zhitkov *et al.* 1994). This work was mainly intended to constrain the physical properties and the age of the kimberlites, because this problem was of interest to the Diamond Exploration Company 'Almazy-Sakha-Rossija'. Although many palaeomagnetic studies of Middle–Late Palaeozoic rocks have been performed in Siberia, most do not meet present-day reliability requirements. A direct consequence is that the apparent polar wander path (APWP) of the Siberian platform remains poorly constrained, thus there is a crucial need for new studies using modern techniques. The most recent compilations of the Siberian data (Van der Voo 1993; Smethurst *et al.* 1998) reveal large uncertainties for the Middle–Late Palaeozoic records. The present study was intended to improve this situation and to contribute to the global palaeomagnetic database for one of the most

* Present address: Physics Department, University of Alberta, Edmonton, AB, Canada, T6G 2J1. E-mail: vkrav@phys.ualberta.ca

significant cratons used in all palaeomagnetic reconstructions. This also provided us with the opportunity of studying traps, because they are the centre of renewed interest in relation to continental break-up and mass extinctions (e.g. Courtillot 1994; Courtillot *et al*. 1999; Dalziel *et al*. 2000).

## GEOLOGICAL SETTING

The Siberian platform consists of a series of Archaean and Proterozoic crustal terranes that were accreted together during the Proterozoic before being subjected to several periods of lithospheric extension (Zonenshain *et al.* 1990; Rosen *et al.* 1994). The position of the Siberian platform is shown in Fig. 1 in the frame of the surrounding folded areas and blocks. The edges of the Siberian platform are depicted for the Precambrian (solid line) and Middle Palaeozoic (dashed line) periods. The north and far-eastern parts of Siberia, including the Taimyr and Verkhoyansk folded belts, existed at that time as passive margins and were folded in Mesozoic times. Palaeomagnetic data from the Omolon block show that accretion with the Siberian platform occurred in post-late Jurassic time (Lozhkina 1981; Savostin *et al*. 1993), resulting in folding of the Verkhoyansk middle Palaeozoic to Mesozoic sediments (Zonenshain *et al*. 1990). The southern edge of the platform lies at the Mongol–Okhotsk suture, which also formed in Mesozoic times (Zonenshain *et al*. 1990; Kravchinsky 1990; Enkin *et al*. 1992; Kravchinsky *et al*. 2001).

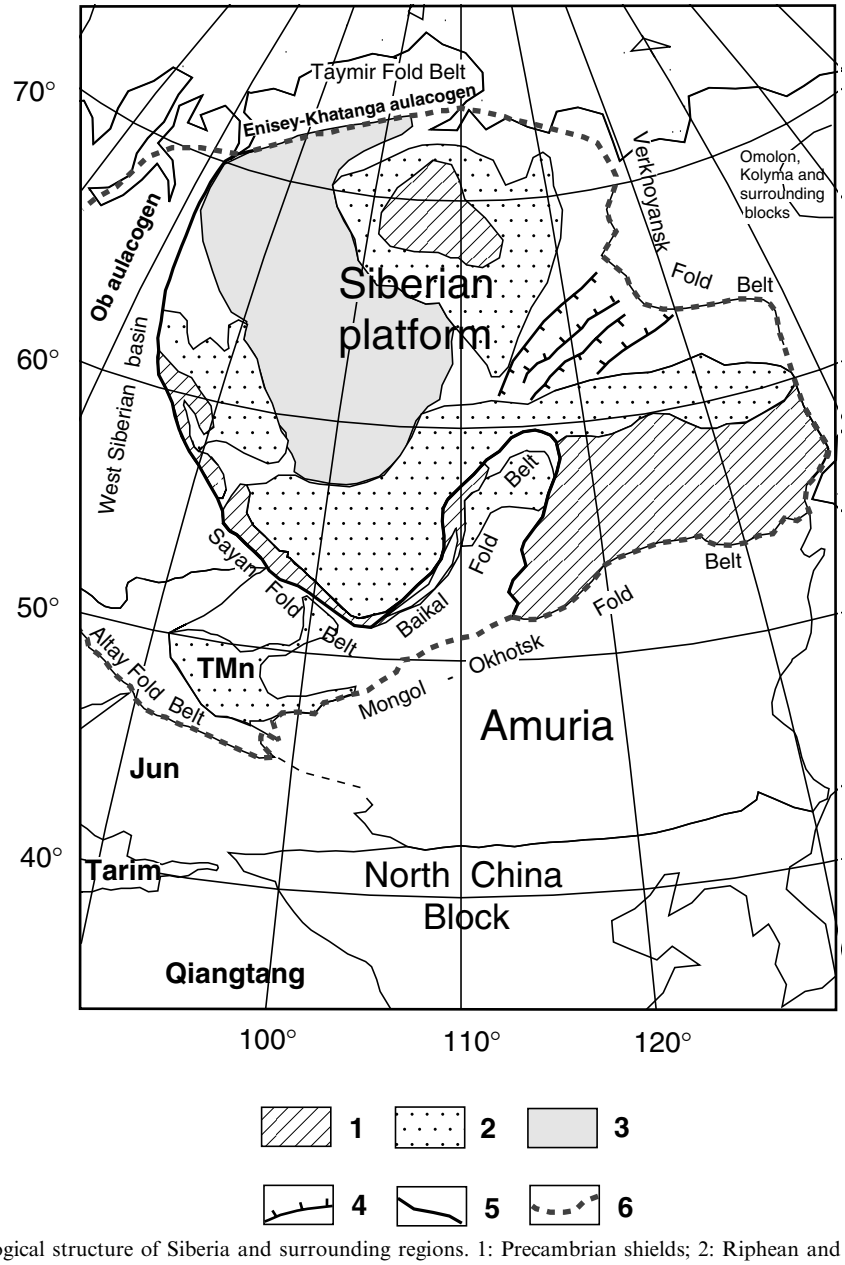


**Figure 1.** Simplified geological structure of Siberia and surrounding regions. 1: Precambrian shields; 2: Riphean and Palaeozoic sediment cover; 3: Permo-Triassic traps; 4: Viluy palaeorift; 5: edge of Precambrian platform; 6: Middle–Late Palaeozoic border of Siberian block. Names of blocks: TMn–Tuva-Mongolian; Jun: Jungar.

A chain of Palaeozoic to Mesozoic kimberlite fields stretches over nearly 1000 km in a SW–NE direction across the north-central part of the platform, and a trail of Mesozoic kimberlites extends 320 km to the northwest from the centre of the platform along the eastern boundary of the Anabar Shield (Fig. 2). The sedimentary cover of the Siberian Platform ranges in thickness from 2 to 2.5 km (Olenek Uplift, Anabar Shield margins) to 12–14 km (Viluy Basin). This cover accumulated from Riphean to Cretaceous times. Sedimentary rocks accumulated in large basins at times of extension. Extension in the Middle Riphean led to the development of the Udzha and Majmecha aulacogens to the east and west of the Anabar Shield. The wide distribution of Riphean, Vendian and lower Palaeozoic sediments on the Siberian platform suggests the presence of other Riphean aulacogens beneath younger deposits (Zonenshain *et al.* 1990). Kimberlite pipes related to the Riphean extension stage are unknown, although the occurrence of pyrope garnets in Palaeozoic beach placers in the SW part of the craton suggests that Precambrian kimberlites may exist (Griffin *et al.* 1999). On the eastern side of the Siberian platform, the Devonian Viluy and Kyutungda aulacogens extend into the platform from the ancient passive margin. All Devonian–Early Carboniferous kimberlite occurrences lie between these aulacogens (Fig. 2). The kimberlites of the Siberian platform were emplaced during three main epochs: in the Devonian–Early Carboniferous, in the Triassic and in the Cretaceous (Krivonos 1997). The Devonian and Triassic kimberlites are linked with corresponding epochs of intraplate basalt volcanism. The exact age relationship of kimberlite and trap magmatism is not well known because of the lack of radiometric data for the traps and large uncertainties for the kimberlites. Cretaceous kimberlites are known in the north of the platform on the slopes of the Olenek uplift. They are probably connected to the intraplate magmatism in the Arctic area (Zonenshain *et al.* 1990). The Viluy aulacogen (Fig. 2) contains 7–8 km of Upper Devonian–Lower Carboniferous rocks alone (evaporites and bimodal

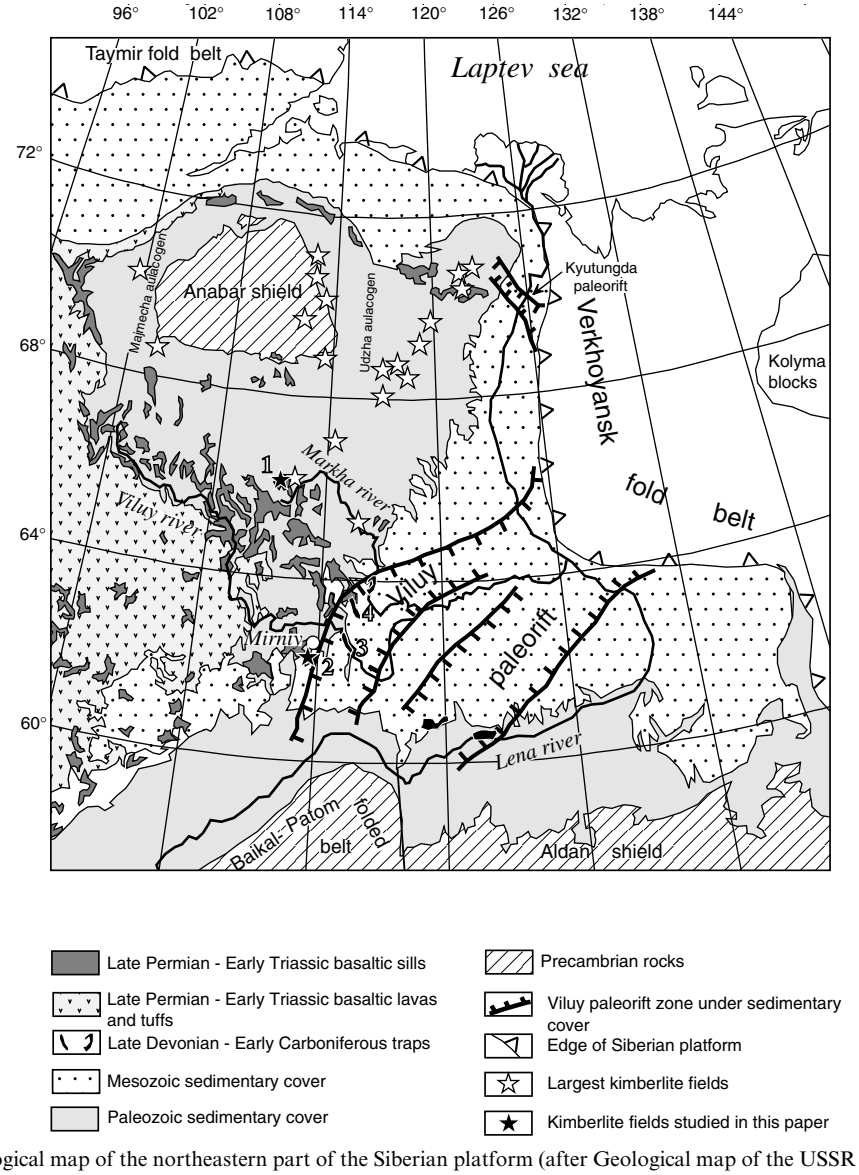


**Figure 2.** Simplified geological map of the northeastern part of the Siberian platform (after Geological map of the USSR 1980,). Sampling localities reported in this paper: 1–Alakit-Markha kimberlite pipes field (Sytikanskaya, Yubileinaya, and Aikhal pipes, Permo-Triassic traps); 2–Malo–Botuoba kimberlite pipe field (Mir and Sputnik pipes); 3–Viluy river Late Devonian–Early Carboniferous traps (sills and dykes); 4–Markha river Late Devonian–Early Carboniferous traps (sills and dykes).

volcanics). The narrow (50 km) Kyutungda aulacogen is filled with Upper Devonian–Lower Carboniferous evaporites (Masaitis *et al.* 1975; Oleinikov 1979; Shpount & Oleinikov 1987).

Radiometric data for the kimberlites and geological age estimates have been summarized in Brakhfogel (1984), Krivonos (1997) and Griffin *et al.* (1999). There are large differences between the age estimates of different pipes obtained by different methods. Griffin *et al.* (1999) emphasized this problem for different kimberlite fields. For instance, these authors indicate that some K–Ar ages are significantly older than other estimations with different methods, and in several cases in contradiction with reliable geological dating, which suggests an excess of argon. Unfortunately, it is presently impossible to date each single kimberlite pipe because of such differences between geological and absolute dating. We list below the information known to us, which may help to date the kimberlite fields that were sampled in this study.

The *Alakit–Markha kimberlite field* is located south of the Anabar shield (kimberlite pipe field number 1 in Fig. 2). Famous kimberlite pipes in this field include Sytikanskaya, Yubileinaya, Aikhal, Komsomol'skaya, etc. The diameters of most of the kimberlite pipes are a few hundred metres. We sampled Sytikanskaya (66.11°N, 111.8°E), Yubileinaya (66.0°N, 111.7°E) and Aikhal (66.17°N, 111.33°E) in quarries. Pipes have a subvertical mode of occurrence. They cut subhorizontally through carbonate and clay-carbonate rocks of Cambrian, Ordovician and Silurian age. Carboniferous–Permian sediments (sandstones) of 15 m thickness cover the Sytikanskaya pipe. The oldest rocks that cover the kimberlites are Middle–Late Carboniferous (Katsk formation). Late Permian–Early Triassic traps cover the Carboniferous–Permian sediments. In some cases, the traps directly overlie the kimberlites. Xenoliths with faunas consisting of brachiopods, tetracorallians, tabulates, ostracods, tentaculites and trilobites of Middle–Late Devonian age were found in the Alakit–Markha kimberlite field (Krivonos 1997). Absolute dating of pipe yields: 364–461 Ma (fission track zircon), 344–358 Ma (U–Pb zircon), $350 \pm 13$ Ma (Rb–Sr, Pipe No. 3) and 335–365 Ma (K–Ar, Moskvichka pipe), thus the age of the field is Late Devonian–Early Carboniferous.

The *Malo–Botuoba kimberlite field* consists of a number of pipes including Mir, Trubka-1, Sputnik, Amakinskaya, Internatsional'naya and Taezhnaya (kimberlite pipe field number 2 in Fig. 2). The Palaeozoic basement sediments of this kimberlite province are exposed close to the Viluy aulacogen, in the centre of the Siberian platform, in the southernmost part of the Anabar Shield. We sampled the Mir and Sputnik kimberlite pipes (coordinates 62.5°N, 113.0°E) at different levels of quarries. These pipes are subvertical and cut Early to Late Cambrian carbonates. Radiometric data are scattered. Fission track zircon ages are mainly between 358 and 397 Ma. U–Pb zircon dating gives ages from 344 to 403 Ma. At the Mir pipe the K–Ar ages are $403 \pm 15$ Ma and the Rb–Sr age is $324 \pm 11$ Ma. Basalt rocks of Late Devonian age were found in xenoliths. The pipe cuts across a Palaeozoic trap sill. Conglomerates of these pipes were found in Carboniferous and Jurassic rocks of the region. Thus, the Late Devonian–Early Carboniferous age of this field is about 355–365 Ma.

*Middle Palaeozoic traps*, both intrusive and extrusive, occur in the eastern part of the Siberian platform. They are well exposed along the Viluy, Markha and Lena rivers, and along some fractures on the slopes of the Anabar and Aldan shields (Fig. 2). The intrusive rocks incorporate dykes, sills and layered basalt breccias. Middle Palaeozoic basalt outcrops have been mapped in several parts of the rifts, often interbedded with ash and tuffs. In most cases, the lavas consist of olivine- and plagioclase-bearing basalts; aphyric varieties are rare (Masaitis *et al.* 1975; Oleinikov 1979; Zolotukhin & Almukhamedov 1988). Traps and sediments of Late Devonian–Early Carboniferous age cover 6–8 km of sediments of Late Proterozoic and Early Palaeozoic, up to Silurian, age. Sills are spread over the central part of the Viluy area. Intrusions under sedimentary cover are spread along the edges of the palaeorifts in association with large regional normal faults. Effusives are common in the lower parts of the sedimentary sections. The Viluy aulacogen extends over 600 km in a NE direction and plunges under the Verkhoyansk fold belt. The trap volume is very large—about 100 000 $km^3$ for those in the Viluy aulacogen alone.

The age of traps constrained by K–Ar absolute dating obtained about 20–30 yr ago has a large scatter from 450 to 320 Ma. Most ages are clustered near 340–380 Ma (Shpount & Oleinikov 1987). Moreover, some dykes have been eroded and covered by Early and Middle–Late Carboniferous sediments. Trap conglomerates are known in sediments with ages younger then Tournaisian. Moreover, all Palaeozoic dykes in this area cut Middle–Late Devonian sediments. Thus we can conclude that the traps have Late Devonian–Early Carboniferous ages (more likely Frasnian–Tournaisian) (377–350 Ma).

We sampled Late Devonian–Early Carboniferous traps along the Viluy and Markha rivers (numbers 3 and 4 in Fig. 2). In this paper, we present data from eight localities, with various occurrences of trap sills and dykes. In some trap sills we measured the bedding orientation of Ordovician interbedded sediments. The dips of these sediments rarely exceed 5°–15°. We also sampled some kimberlite pipes with a Middle Palaeozoic age in the same region.

*Permo-Triassic traps* occupy the western part of the Siberian platform. Two major lower Triassic rift zones are known to the west and north of the Siberian Platform, the Ob aulacogen under the West Siberian basin and the Yenisey–Khatanga aulacogen under the same basin (Fig. 1). The total thickness of the volcanic sequence is about 5 km, with a total present volume of the order of 1 400 000 $km^3$. It is now known that most of these traps were formed during a brief interval possibly less than 1 Myr in duration at the Permo-Triassic boundary, i.e. $250 \pm 1.6$ Ma (Renne & Basu 1991; Campbell *et al.* 1992; Renne *et al.* 1995; Venkatesan *et al.* 1997; Hofmann 1997). The thickness of sedimentary rocks reaches 13 km; the superdeep Tumen drilling well (7.5 km) penetrated more than 1000 m of Lower Triassic tholeiitic basalts. Griffin *et al.* (1999) proposed that these aulacogens represent two branches of a triple-junction rift system related to the eruption of the Siberian Traps (see also Courtillot *et al.* 1999), with a possible 'hotspot' or plume head located at the intersection of the aulacogens. The Permo-Triassic Siberian trap magmatism was apparently not associated with plate boundaries, but it was linked with lithospheric break-up (Almukhamedov *et al.* 1996; Courtillot *et al.* 1999). Almukhamedov *et al.* (1996) propose that the first two periods of magmatism in the Noril'sk area of the Siberian traps were connected with rifting and the third one with lithospheric break-up. Several Early Triassic aulacogens linked to rifting have been revealed by deep drilling in western Siberia and are linked to trap magmatism and continental rifting (Surkov *et al.* 1993; Almukhamedov *et al.* 1996). The superdeep holes

penetrate the entire sedimentary Mesozoic–Cenozoic cover and into lower–middle Triassic basalts below depths of about 5700–6000 m (Nesterov *et al.* 1995). According to these authors these sediments corresponded to continental 'lake and plain' landscapes, not to oceanic sedimentary basins, as suggested on the basis of geophysical data only (Aplonov 1987). Zonenshain *et al.* (1990) consider the possibility that an Ob palaeo-ocean existing during the Triassic. Opening of this ocean might have been related to flood basalt magmatism. There is a belt of Early Triassic alkali–ultramafic intrusions with carbonatites in the west of the Anabar Shield, younger than the Siberian traps (Zonenshain *et al.* 1990; Griffin *et al.* 1999).

For the present study, we sampled three Permo-Triassic trap sills (5–20 m thick) that overlie kimberlites or sediments in the areas of the Sytikanskaya, Yubileinaya and Aikhal pipes. This is the most eastern occurrence of Permo-Triassic flood basalts on the Siberian platform. Basalt dykes cut across Carboniferous–Permian sediments in our study region and their age is doubtlessly Permo-Triassic.

## PALAEOMAGNETIC RESULTS

We sampled oriented blocks, from which we cut from two to five oriented 8 $cm^3$ cubic samples. A total of 400 samples from different hand blocks were studied from 58 sites and 17 localities. Except for some Palaeozoic traps of the Viluy and Markha rivers, all directions were calculated using only *in situ* coordinates in the absence of any folding on the Siberian platform.

Stepwise thermal demagnetizations and magnetic measurements of the samples were carried out in the Irkutsk palaeomagnetic laboratory (80 per cent of the samples) and in the palaeomagnetic laboratory of the Institut de Physique du Globe de Paris (IPGP; 20 per cent of the samples). Tables in this paper include two statistical levels: site averages based on samples and locality averages based on sites.

Thermal demagnetization was performed in Irkutsk using ovens housed in three concentric μ-metal shields. The residual field is about 10 nT in the centre of the ovens. The samples were demagnetized in 10–50 °C steps up to 600–650 °C, and the remanent magnetization was measured with a JR-4 spinner magnetometer. Magnetic susceptibility was measured with a KLY-2 Kappabridge (Irkutsk) and a Molspin susceptibility meter (Paris). In Paris, we used a Pyrox oven with about 4–6 nT residual field, an alternating field Schonstedt demagnetizer, a JR-5 spinner magnetometer and two-axis horizontal and vertical cryogenic magnetometers. Data were processed using Vinarsky *et al.*'s (1987) OPAL software, Enkin's (1996) palaeomagnetic data treatment software and the Cogné (2000) PALEOMAC software. In all cases, Zijderveld (1967) diagrams were constructed for each sample, results were analysed using principal component analysis (Kirschvink 1980), and site-mean directions were calculated using Fisher (1953) statistics. For mixed populations of directions and remagnetization great circles with sector constraints (Halls 1976; McFadden & McElhinny 1988), we used the combined analysis technique of McFadden & McElhinny (1988).

Isothermal remanent magnetization (IRM) experiments, thermomagnetic curves [Curie point measurements, $J_s(T)$] and hysteresis loops were performed in the palaeomagnetic laboratory of the Munich Institute of Applied Geophysics.

### Kimberlite pipes of Late Devonian–Early Carboniferous age

#### *Rock-magnetic properties of kimberlites*

Some rock-magnetic parameters such as NRM (natural remanent magnetization) intensity, magnetic susceptibility and Koenigsberger ratio are listed in Table 1. Basically three different types of behaviour have been observed, as illustrated by the three samples in Fig. 3. The first types (a and b) were

**Table 1.** Rock-magnetic properties of studied kimberlites and traps on a locality level.

| Locality | *n* | NRM (ε) | Kappa (ε) | *Q* (ε) |
|---|---|---|---|---|
| 1 Sytikanskaja kimberlite pipe | 244 | 285 (1.12) | 870 (1.11) | 0.54 (1.09) |
| 2 Yubileinaja kimberlite pipe | 141 | 370 (1.1) | 3100 (1.04) | 0.2 (1.08) |
| 3 Aikhal kimberlite pipe | 84 | 30 (1.15) | 170 (1.15) | 0.33 (1.09) |
| 4 Satellite of Aikhal kimberlite pipe | 82 | 4.4 (1.10) | 22 (1.06) | 0.41 (1.05) |
| 4 Mir kimberlite pipe | 474 | 190 (1.06) | 300 (1.05) | 1.32 (1.03) |
| 5 Sputnik kimberlite pipe | 169 | 36 (1.22) | 75 (1.14) | 0.83 (1.12) |
| 6 Late Devonian–Early Carboniferous traps of Markha river region | 180 | 790 (1.05) | 2140 (1.02) | 0.77 (1.05) |
| 7 Late Devonian–Early Carboniferous traps of Viluy river region | 230 | 370 (1.06) | 1240 (1.04) | 0.62 (1.04) |
| 8 Late Devonian–Early Carboniferous traps of Mir pipe area | 20 | 0.06 (1.2) | 0.2 (1.5) | 0.17 (1.3) |
| 9 Late Permian–Early Triassic traps of Sytikanskaja pipe area | 15 | 1080 (1.24) | 1070 (1.16) | 1.65 (1.12) |
| 10 Late Permian–Early Triassic traps of Yubileinaja pipe area | 10 | 6630 (1.16) | 2415 (1.05) | 4.50 (1.2) |
| 11 Late Permian–Early Triassic traps of Aikhal pipe area | 11 | 2780 (1.14) | 1360 (1.03) | 3.35 (1.14) |

n: number of samples accepted for calculation; NRM: natural remanent magnetization intensity (mA $m^{-1}$); Kappa: magnetic susceptibility ($10^{-5}$ SI units); Q: Koenigsberger ratio ($Q$ = NRM/(Kappa $T$), where $T$ is the Earth's magnetic field value in the studied region; ε: standard factor of log-normal distribution.

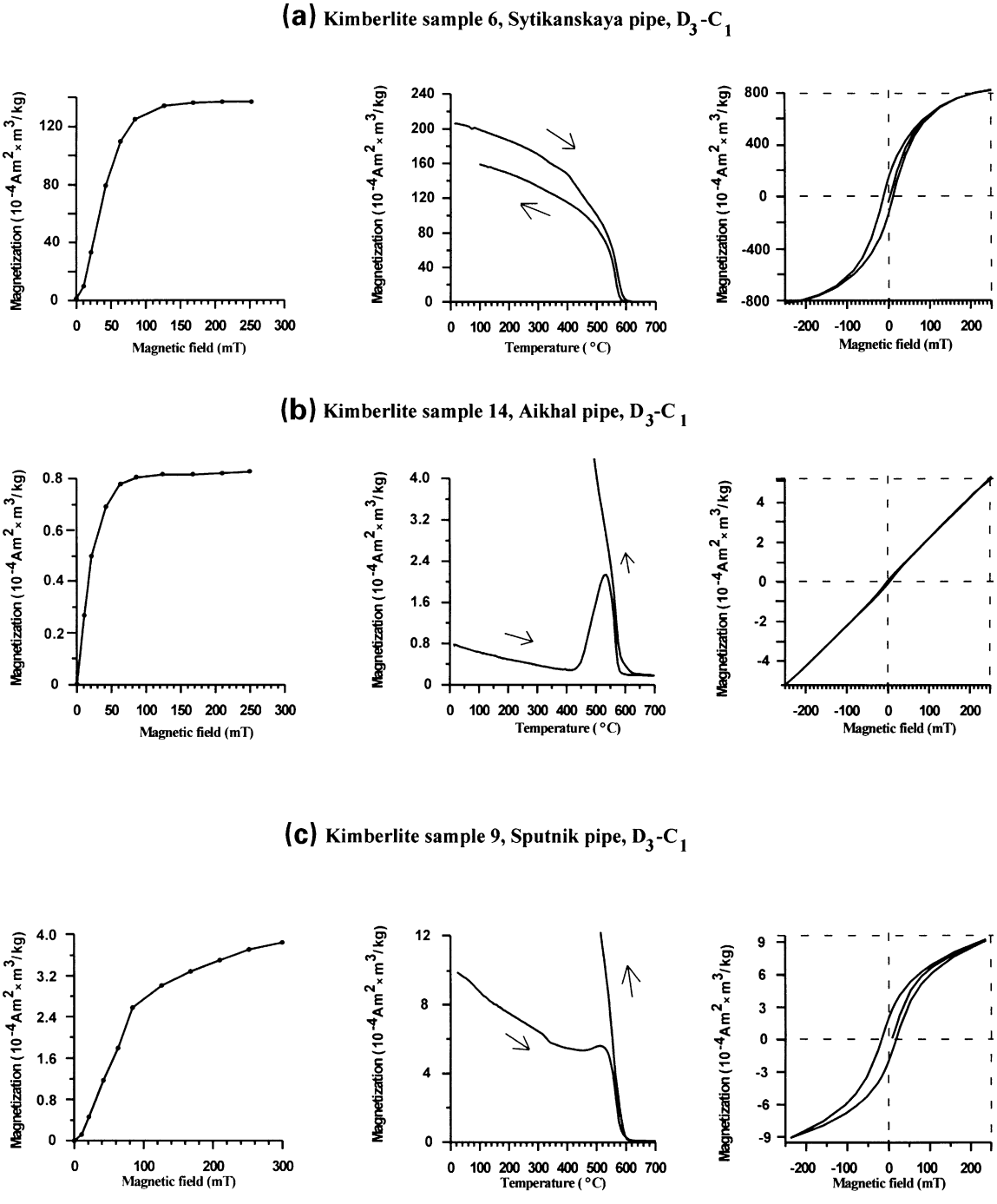


**Figure 3.** Typical results of rock magnetic experiments for kimberlite samples from the Sytikanskaya and Aikhal (Alakit–Markha field) and Sputnik (Malo–Botuoba) pipes. Isothermal remanent magnetization (IRM) acquisition curves (left), Curie point thermomagnetic curves $J_s$(T) (centre) and hysteresis loops (right).

obtained for all studied pipes. A third type of behaviour (c) was only observed for the kimberlites from the Mir and Sputnik pipes, i.e. the Malo–Botuoba kimberlite field. In the first case (sample 6) saturation is attained at 100–120 mT. The thermomagnetic curves are almost reversible with a Curie temperature of 580 °C. The shape of the hysteresis curve is compatible with a relatively narrow distribution of single- or pseudo-single-domain grains. We infer that this sample is dominated by magnetite. The magnetization of the second sample saturates in a low field (50 mT). In contrast to the previous case there is a marked increase of magnetization beyond 400 °C, which is typical of the transformation of titanomagnetite into magnetite. During transformation, the parent spinels evolve towards magnetite and the Curie point rises (Dunlop & Ozdemir 1997). There is almost no hysteresis, which explains the low intensity of the remanence.

SIRM acquisition of the third sample indicates the presence of two components with intermediate and high coercivities, respectively. These could be related to the presence of sulphides such as pyrrhotite. The thermomagnetic results show a large

production of a strongly magnetic component during the first stage of cooling, which is presumably magnetite. Because the initial magnetization is not linked with magnetite, the NRM results from the pipe must be considered with extreme caution.

*Kimberlites from the Sytikanskaya pipe*

The vast majority of the 64 samples from nine sites showed two magnetization components. The low-temperature component (LTC), with a north and down direction (Fig. 4), averages $D=341.8°$, $I=83.0°$ ($k=29.0$, $\alpha_{95}=10.5°$, $N=8$ sites; Fig. 4, Table 2) in geographical coordinates, identical to the present-day geomagnetic field direction in the region ($D=353.2°$, $I=81.3°$).

The high-temperature component (HTC) unblocks between 150 and 600 °C (Fig. 4, Table 2). In a few cases, magnetic susceptibility increased during demagnetization, and directions became unstable. This probably reflects the similar increase in $J_s$ depicted in Fig. 3, which was interpreted as a conversion of titanomagnetite into magnetite. The Fisherian average at the site level is $D=298.1°$, $I=-60.7°$ ($k=27.0$, $\alpha_{95}=10.1°$, $N=9$ sites). There is no folding in the central part of the Siberian platform, and therefore no fold test can be applied. All samples have reversed HTC polarity (Fig. 4b).

*Sediments from contact with Sytikanskaya kimberlite pipe*

The Sytikanskaya kimberlite pipe intrudes carbonate and fine sandstone sediments of Late Cambrian age, which were also studied. The sediment samples were taken 50 m away from the contact (the size of the kimberlite pipe is about $300\times800$ m). The LTC component calculated from 20 samples ($D=323.2°$, $I=-82.0°$, $k=14.5$, $\alpha_{95}=8.9°$; Fig. 4c, Table 3) is close to the average direction of the HTC of the kimberlites, but the $\alpha_{95}$ confidence intervals do not intersect (Fig. 4). This LTC may result from partial overprinting related to kimberlite emplacement. This is a form of baked-contact test, which would argue in favour of the primary character of the kimberlite HTC. The emplacement temperature of kimberlites is both variable and debated (i.e. Van Fossen & Kent 1993). Some authors argue in favour of a 'cold' emplacement temperature, which would limit the overprinting effects, but other cases of kimberlite-related remagnetization (thermochemical) can also occur. The sediment HTC does not converge towards the origin of the Zijderveld diagrams and sometimes displays complex behaviour. We could not isolate any stable, consistent component at high temperatures.

*Kimberlites from the Yubileinaya pipe*

Two characteristic components were isolated at five sites from the Yubileinaya kimberlite pipe (Fig. 5). LTC has an average direction $D=13.6°$, $I=82.0°$ ($k=7.3$, $\alpha_{95}=12.0°$, $N=23$ samples; Fig. 5, Table 4). It is again close to the present field direction in the region and we interpret it as present-day overprint. An HTC could be isolated between 200 and 300 °C and 600 and 625 °C, which converges with the origin of the Zijderveld diagrams. The average direction $D=301.0°$, $I=-56.8°$ ($k=42.4$, $\alpha_{95}=11.9°$) from five sites (Fig. 5, Table 4) is close to the average direction of kimberlites from the Sytikanskaya pipe and also has reversed polarity.

**Table 2.** Site-mean palaeomagnetic directions for the low- and high-temperature components of magnetization of Sytikanskaya kimberlite pipe (66.11°N, 111.8°E).

| Site number | *n* | *D*g (°) | *I*g (°) | *D*s (°) | *I*s (°) | *k* | $\alpha_{95}$ (°) |
|---|---|---|---|---|---|---|---|
| Low-temperature component | | | | | | | |
| Stk-1 | 2 | 85.7 | 80.3 | – | – | – | – |
| Stk-2 | 4 | 327.3 | 86.2 | – | – | 28.8 | 17.4 |
| Stk-3 | 6 | 320.5 | 58.0 | – | – | 6.6 | 28.3 |
| Stk-5 | 3 | 72.6 | 73.4 | – | – | 64.6 | 15.5 |
| Stk-6 | 5 | 55.0 | 77.9 | – | – | 14.1 | 21.1 |
| Stk-7 | 6 | 265.3 | 81.9 | – | – | 14.9 | 18.0 |
| Stk-8 | 6 | 305.9 | 75.6 | – | – | 71.7 | 8.0 |
| Stk-9 | 6 | 298.7 | 76.9 | – | – | 46.0 | 10.0 |
| Overall mean | 8 sites | 341.8 | 83.0 | – | – | 29.0 | 10.5 |
| High-temperature component | | | | | | | |
| Stk-1 | 6 | 330.0 | −63.9 | – | – | 8.0 | 25.3 |
| Stk-2 | 8 | 301.2 | −62.8 | – | – | 8.5 | 20.2 |
| Stk-3 | 10 | 5.2 | −76.5 | – | – | 9.6 | 16.4 |
| Stk-4 | 10 | 319.4 | −62.5 | – | – | 4.3 | 26.4 |
| Stk-5 | 4 | 290.3 | −51.7 | – | – | 74.5 | 11.4 |
| Stk-6 | 5 | 287.8 | −43.7 | – | – | 51.7 | 11.1 |
| Stk-7 | 9 | 287.0 | −57.7 | – | – | 6.7 | 21.5 |
| Stk-8 | 6 | 298.7 | −52.6 | – | – | 12.4 | 23.2 |
| Stk-9 | 6 | 261.6 | −56.0 | – | – | 8.8 | 24.2 |
| Overall mean | 9 sites | 298.1 | −60.7 | – | – | 27.0 | 10.1 |

*n*: number of directions for samples or sites accepted for calculation; *D* (*I*): declination (inclination) of characteristic component of NRM in geographical (g) or stratigraphic (s) system of coordinates; *k*, $\alpha_{95}$: precision parameter and half-angle radius of the 95 per cent probability confidence cone.

**Table 3.** Mean palaeomagnetic direction for the low-temperature component of magnetization of the Late Cambrian limestones and fine sandstones near the contact with the Sytikanskaya kimberlite pipe (Late Devonian–Early Carboniferous) (66.11°N, 111.80°E).

| *n* | *D*g (°) | *I*g (°) | *D*s (°) | *I*s (°) | *k* | $\alpha_{95}$ (°) |
|---|---|---|---|---|---|---|
| 20 | 323.2 | −82.0 | – | – | 14.5 | 8.9 |

Same abbreviations as in Table 2.

**Table 4.** Site-mean palaeomagnetic directions for the low- and high-temperature components of magnetization of the Yubileinaya kimberlite pipe (Late Devonian–Early Carboniferous) (66.0°N, 111.7°E).

| Site number | *n* | *D*g (°) | *I*g (°) | *D*s (°) | *I*s (°) | *k* | $\alpha_{95}$ (°) |
|---|---|---|---|---|---|---|---|
| Low-temperature component | | | | | | | |
| Overall mean | 23 | 13.6 | 82.0 | – | – | 7.3 | 12.0 |
| High-temperature component | | | | | | | |
| Yub-1 | 6 | 311.5 | −51.3 | – | – | 12.7 | 19.8 |
| Yub-2 | 8 | 283.4 | −69.3 | – | – | 23.2 | 11.9 |
| Yub-3 | 6 | 319.0 | −51.0 | – | – | 41.4 | 10.5 |
| Yub-4 | 6 | 294.1 | −47.0 | – | – | 11.5 | 21.0 |
| Yub-5 | 4 | 286.5 | −61.7 | – | – | 20.2 | 22.2 |
| Overall mean | 5 sites | 301.0 | −56.8 | – | – | 42.4 | 11.9 |

Same abbreviations as in Table 2.

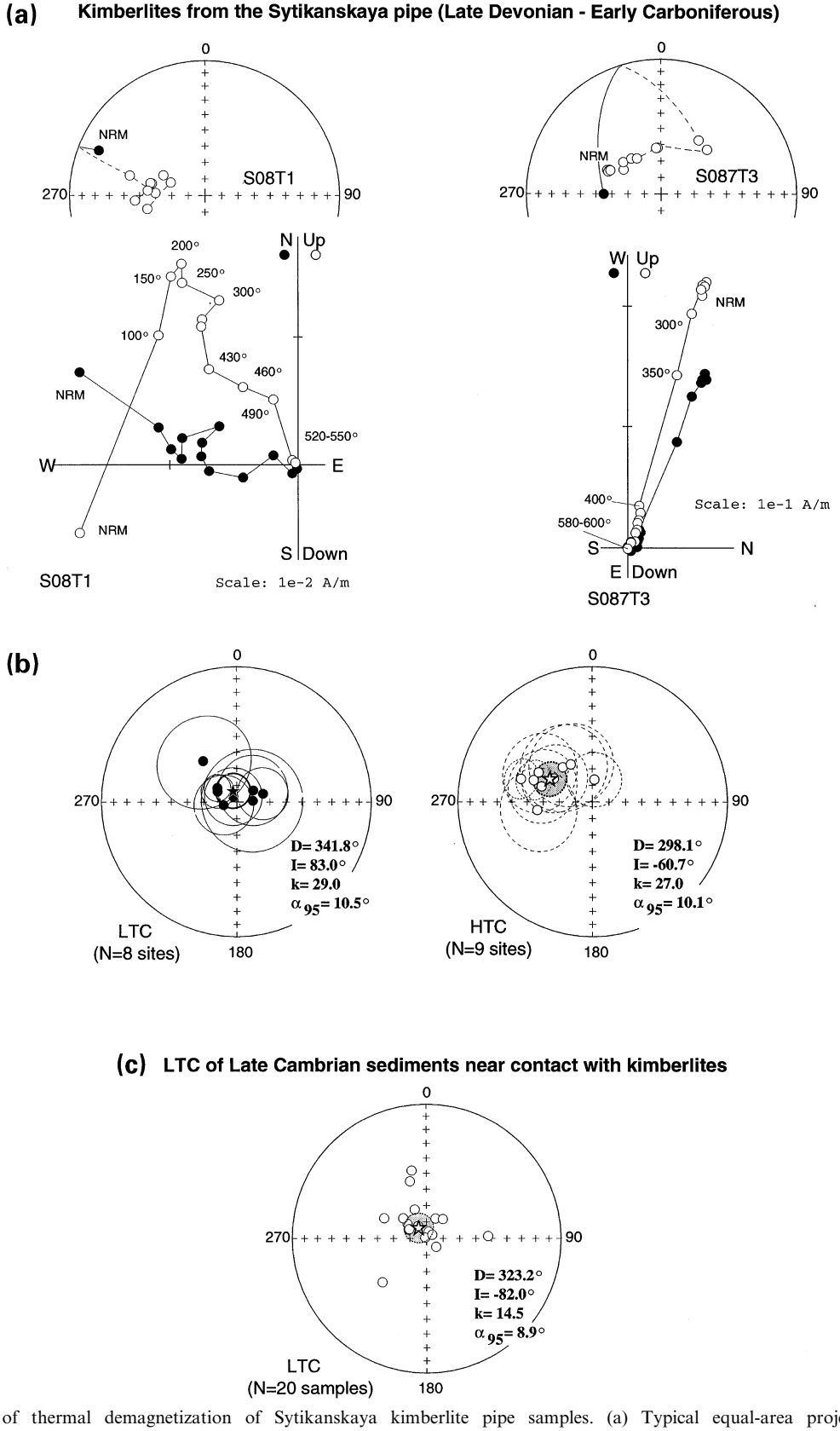


**Figure 4.** Results of thermal demagnetization of Sytikanskaya kimberlite pipe samples. (a) Typical equal-area projections illustrating demagnetization paths during experiments (top) and thermal demagnetization orthogonal vector plots in *in situ* coordinates (Zijderveld 1967). Closed (open) symbols in orthogonal plots: projections onto the horizontal (vertical) plane; temperature steps are indicated in °C. (b) Equal-area projections of site-mean directions of the LTC and HTC, with circles of 95 per cent confidence for the Sytikanskaya kimberlite pipe (Late Devonian–Early Carboniferous). (c) Late Cambrian sediments near contact with kimberlites of the Sytikanskaya pipe (baked test). Closed (open) symbols: downward (upward) inclinations. Star: formation mean directions. All *in situ* coordinates.

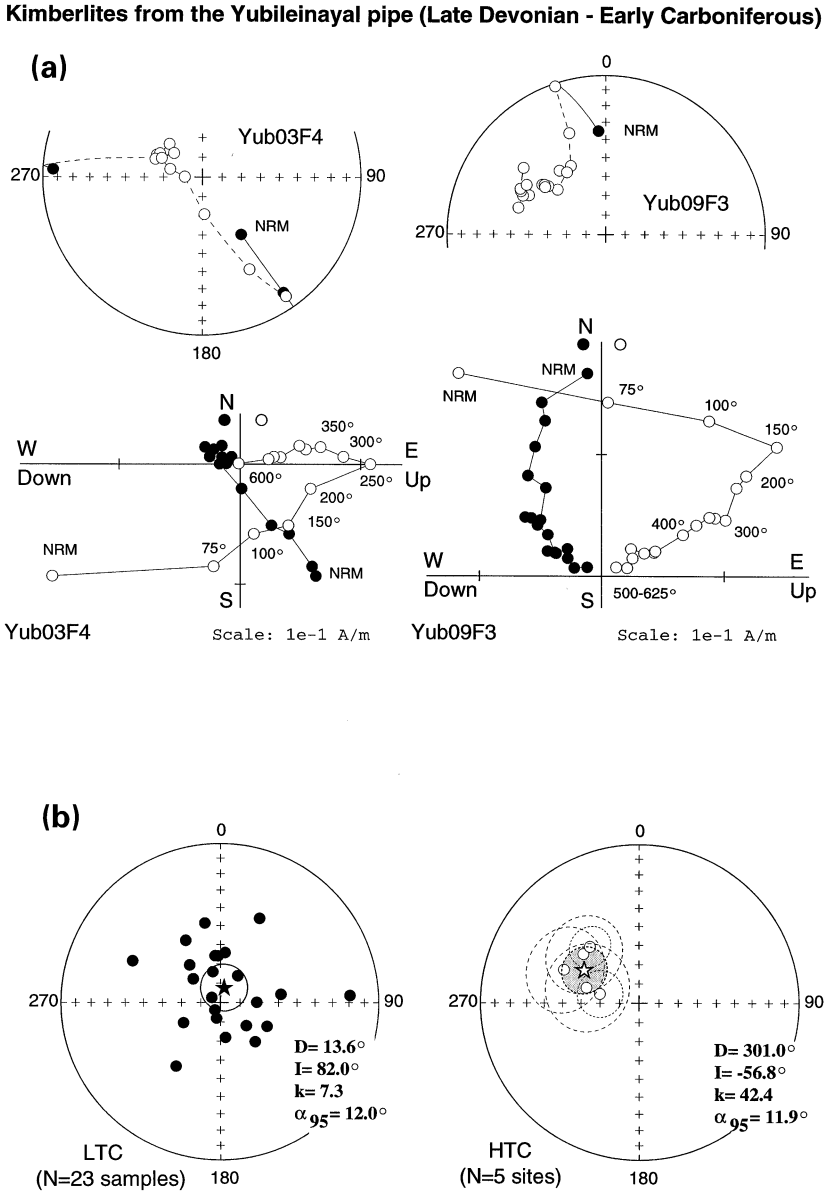


**Figure 5.** (a) Results of thermal demagnetization of Yubileinaya kimberlite pipe samples. (b) Equal-area projections of site-mean directions of LTC and HTC, with circles of 95 per cent confidence for the Yubileinaya kimberlite pipe (Late Devonian–Early Carboniferous). See Fig. 4 legend for further details.

*Kimberlites from the Aikhal pipe and satellite dyke*

Thermal and AF demagnetizations applied to the kimberlite samples of the Aikhal pipe and to a satellite kimberlite body 3 km away from the main pipe isolated two components. The LTC was demagnetized above 250 °C (and sometimes up to 400 °C) and 25 mT (Figs 6a and 7a). The average direction of 22 samples from the Aikhal pipe is $D=59.7°$, $I=67.7°$ ($k=13.3$, $\alpha_{95}=8.8°$) (Fig. 6b, Table 5). This direction does not coincide with the direction of the present geomagnetic field (PGF) in the sampling region, nor with the mean HTC of the Upper Permian–Early Triassic traps, which overlie the pipe (see below). In this case, the LTC may be a complex superposition of several overprints, including both the PGF and the trap HTC. It may lead to the presence of an intermediate temperature component in some samples. However, this component could not always be analysed properly. The LTC of the satellite dyke near Aikhal pipe has an average direction $D=317.0°$, $I=88.3°$ ($k=38.1$, $\alpha_{95}=6.1°$, $N=16$ samples; Fig. 7b, Table 6). This direction coincides with the present geomagnetic field direction. This may be due to the fact that the kimberlite dyke lies further away from the influence of the Permo-Triassic trap sill. The pipe itself is covered by this sill.

The HTC could be isolated (that is, extracted in the unblocking field or temperature range in which it was disturbed by overprints) between 25 and 80 mT and 250 and 500 °C (Figs 6 and 7). During heating to higher temperatures there is a significant increase in magnetic susceptibility. This may be due to oxidation of the titanomagnetite. We therefore used remagnetization circles (Halls 1976). The average direction was observed by combining directions and great circles (McFadden & McElhinny 1988). The mean direction of the HTC is $D=318.9°$, $I=-33.9°$ ($k=9.0$, $\alpha_{95}=11.2°$, $N=21$ samples) for the Aikhal pipe kimberlites (Fig. 6, Table 5), and $D=325.1°$, $I=-38.9°$

**Table 5.** Site-mean palaeomagnetic directions for the low- and high-temperature components of magnetization of the Aikhal kimberlite pipe (66.17°N, 111.33°E).

| Site number | *n* | *D*g (°) | *I*g (°) | *D*s (°) | *I*s (°) | *k* | $\alpha_{95}$ (°) | Notes |
|---|---|---|---|---|---|---|---|---|
| Low-temperature component | | | | | | | | |
| Overall mean | 22 | 59.7 | 67.7 | – | – | 13.3 | 8.8 | |
| High-temperature component | | | | | | | | |
| Overall mean | 21 | 318.9 | −33.9 | – | – | 9.0 | 11.2 | 15d6cc |

*n*: number of directions for samples or sites accepted for calculation; *D* (*I*): declination (inclination) of characteristic component of NRM in geographical (g) or stratigraphic (s) system of coordinates; *k*, $\alpha_{95}$: precision parameter and half-angle radius of the 95 per cent probability confidence cone. Entry d or cc in Notes means number of directions or great circles accepted for calculations; if there is no entry this means that only directions were accepted for calculations.

**Table 6.** Site-mean palaeomagnetic directions for the low- and high-temperature components of magnetization of the satellite body in the area of the Aikhal kimberlite pipe (66.17°N, 111.33°E).

| Site number | *n* | *D*g (°) | *I*g (°) | *D*s (°) | *I*s (°) | *k* | $\alpha_{95}$ (°) | Notes |
|---|---|---|---|---|---|---|---|---|
| Low-temperature component | | | | | | | | |
| Overall mean | 16 | 317.0 | 88.3 | – | – | 38.1 | 6.1 | |
| High-temperature component | | | | | | | | |
| Overall mean | 14 | 325.1 | −38.9 | – | – | 17.6 | 9.9 | 8d6cc |

Same abbreviations as in Table 5.

for the satellite body ($k=17.6$, $\alpha_{95}=9.9°$, $N=14$ samples; Fig. 7, Table 6). Both directions lying close to each other, we infer that both kimberlite bodies were probably formed at the same time.

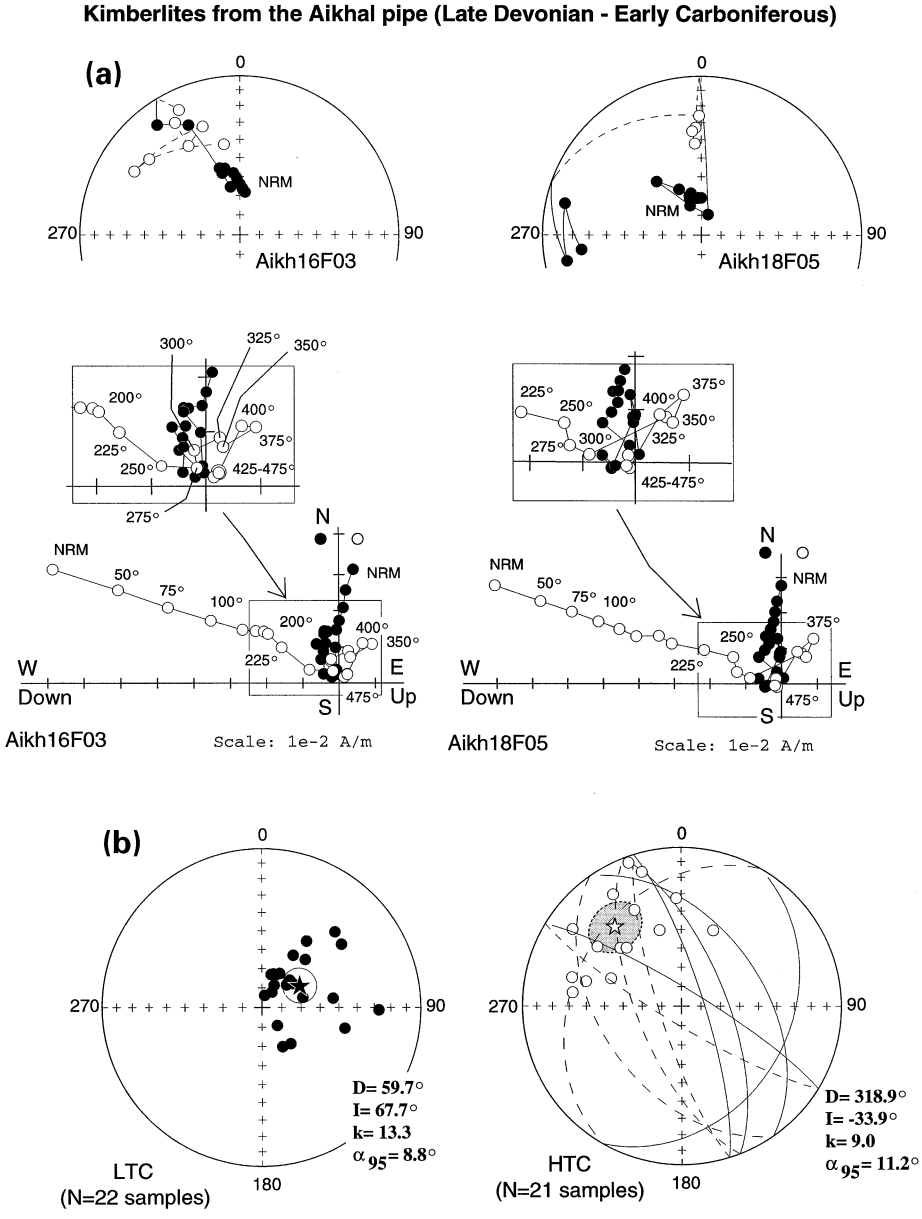


**Figure 6.** (a) Results of thermal demagnetization of Aikhal kimberlite pipe and satellite body samples. (b) Equal-area projections of site-mean directions of LTC and HTC, with circles of 95 per cent confidence for the Aikhal kimberlite pipe (Late Devonian–Early Carboniferous). See Fig. 4 legend for further details.

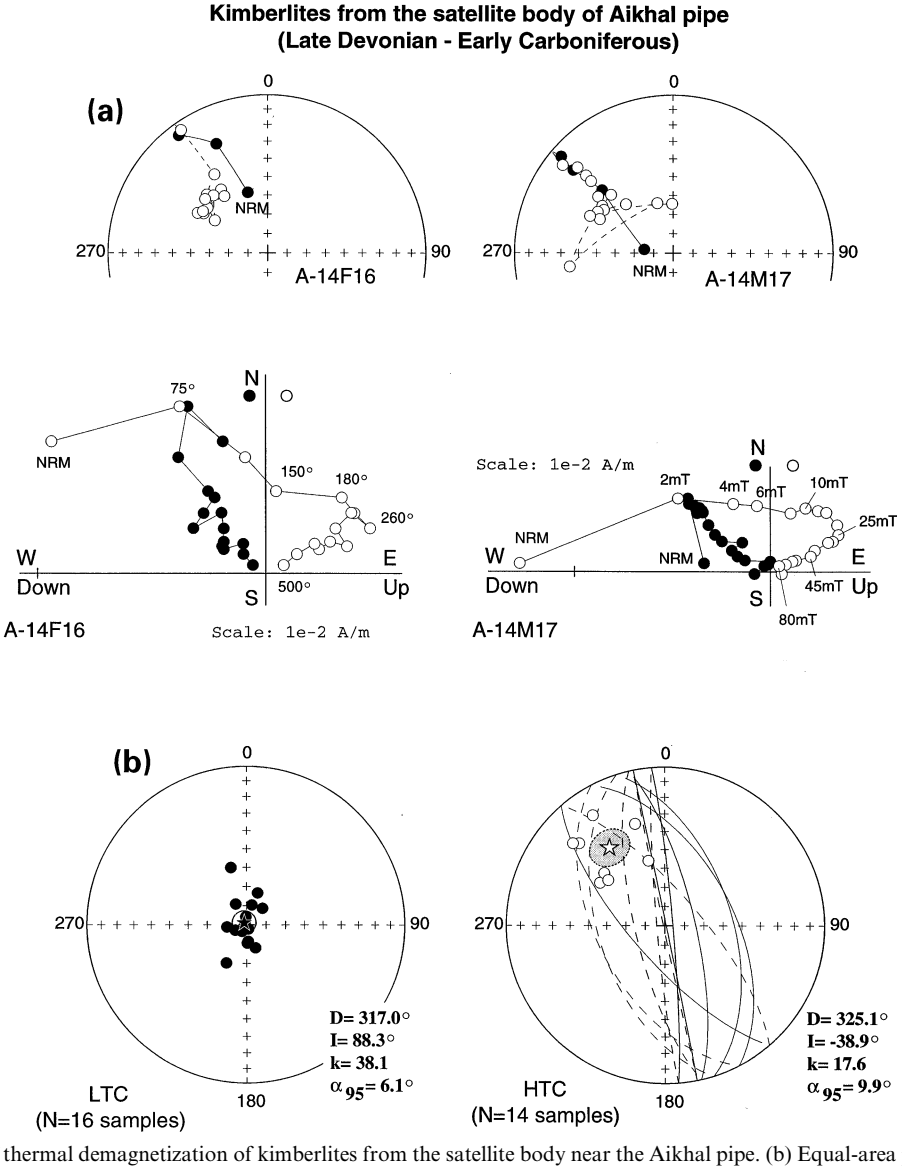


**Figure 7.** (a) Results of thermal demagnetization of kimberlites from the satellite body near the Aikhal pipe. (b) Equal-area projections of site-mean directions of LTC and HTC, with circles of 95 per cent confidence for the satellite kimberlite body (Late Devonian–Early Carboniferous). Other details as in Fig. 4.

### Siberian traps of Late Devonian–Early Carboniferous age

Thermal demagnetization isolated two components for all sill and dyke localities. The LTC is well defined within the intervals NRM to 300 °C and NRM to 25 mT. The LTC direction trends north and down in *in situ* coordinates and does not decay towards the origin (Figs 8 and 9). For the nine sites, the $k$ precision parameter decreases from 265 to 59 after tilt correction. The ratio of precision parameters ($ks/kg = 0.22$) is lower than the critical value at the 95 per cent confidence level (2.69), and thus the fold test (McElhinny 1964) is negative. The post-folding magnetization site-mean direction is $D = 337.8°$, $I = 82.8°$ ($k = 264.6$, $\alpha_{95} = 3.7°$, $N = 7$ localities; Fig. 10, Table 7). However, there are no large differences in bedding orientation of rocks in the Viluy and Markha river areas. Both *in situ* and tilt-corrected directions have comparable statistical parameters, yet the fold test demonstrates significant folding in the centre of the Siberian

**Table 7.** Late Devonian–Early Carboniferous basalt flows and dykes mean directions of the low-temperature component of magnetization for the Markha and Viluy river traps (region around 63.5°N, 116.0°E).

| Locality | $n$ | $D$g (°) | $I$g (°) | $D$s (°) | $I$s (°) | $k$ | $\alpha_{95}$ (°) |
|---|---|---|---|---|---|---|---|
| Markha 2 | 11 | 334.4 | 77.8 | 334.4 | 77.8 | 47.9 | 6.7 |
| Markha 4 | 18 | 343.9 | 79.7 | 343.9 | 79.7 | 24.2 | 7.2 |
| Markha 5 | 21 | 41.7 | 85.2 | 139.0 | 83.0 | 69.5 | 3.8 |
| Markha 6 | 16 | 351.1 | 81.9 | 215.6 | 88.9 | 32.1 | 6.6 |
| Viluy 6 | 10 | 277.3 | 88.1 | 94.7 | 73.9 | 33.0 | 8.5 |
| Viluy 7 | 23 | 309.1 | 82.4 | – | – | 140.0 | 2.6 |
| | | – | – | 72.0 | 77.4 | 145.7 | 2.5 |
| Viluy 8 | 16 | 330.8 | 79.9 | – | – | 52.5 | 5.1 |
| | | – | – | 58.5 | 74.8 | 48.4 | 5.4 |
| Overall | 7 | 337.8 | 82.8 | – | – | 264.6 | 3.7 |
| mean | localities | – | – | 55.5 | 83.6 | 59.2 | 7.9 |

Same abbreviations as in Table 2.

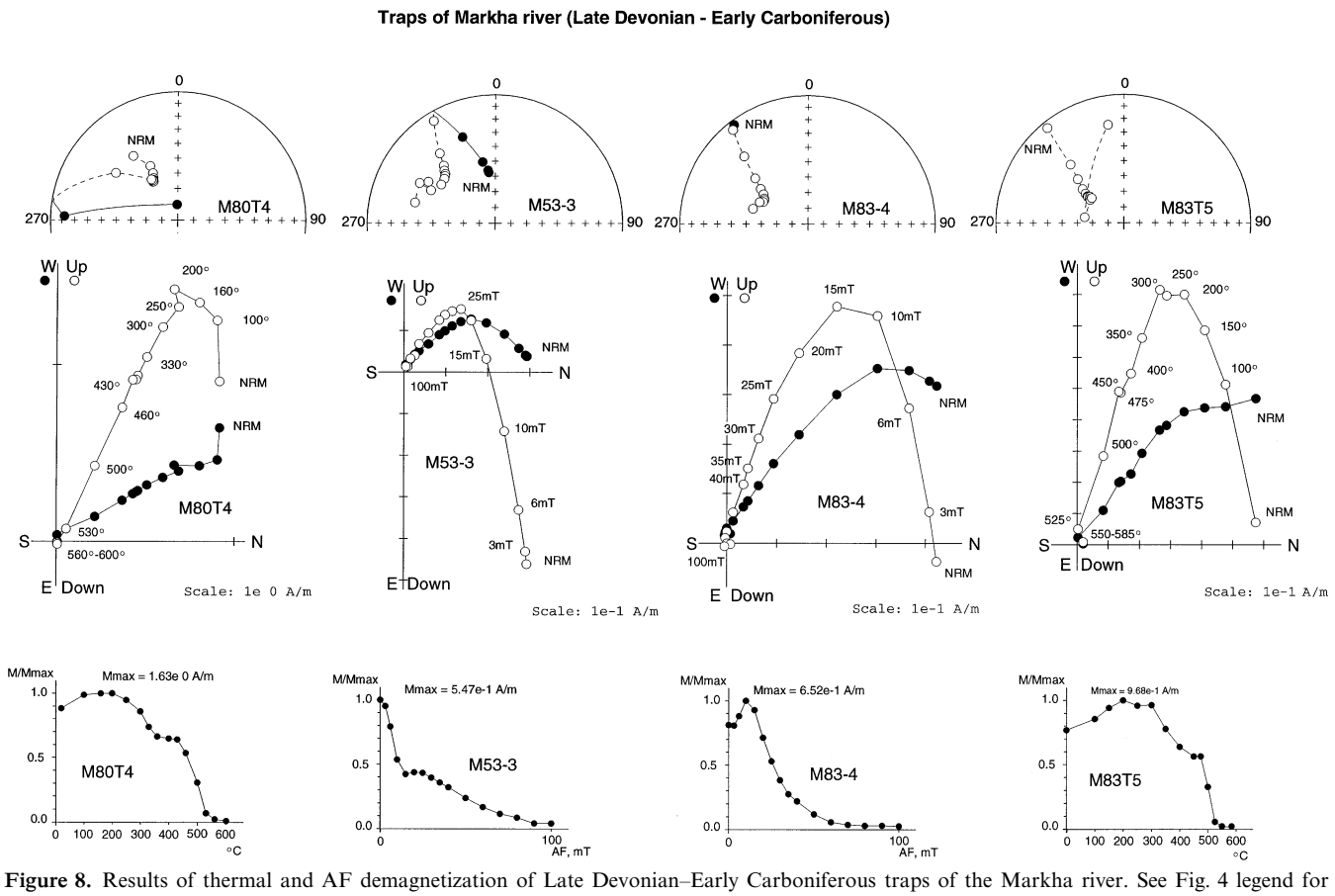


**Figure 8.** Results of thermal and AF demagnetization of Late Devonian–Early Carboniferous traps of the Markha river. See Fig. 4 legend for further details.

platform. In the field we measured very small dips (5°–15°) for some Palaeozoic sediments. This may be due to slight tilting of the sediments on a slope of the Viluy rift during the opening phases. We consider the LTC direction as a present-day (or recent) overprint because this direction is close to the present field direction in the region ($D=349°$, $I=79°$).

The HTC may be isolated in the temperature range between 300 and 430 °C and 580 and 590 °C for all samples (Figs 8 and 9). Stepwise saturation of IRM indicates coercivities between 0.1 and 0.15 T. The thermomagnetic curves are reversible and show a large decrease in magnetization near 585 °C. These observations suggest that magnetite is the carrier of the remanence (Fig. 11).

The HTC converges towards the origin of the demagnetization diagrams. For the large majority of samples the characteristic component was calculated using principal component analysis. The great-circles method with sector constraints was only used for the Markha-2 dyke (for 10 out of 12 samples). We show all HTC mean directions for Late Devonian–Early Carboniferous kimberlite and trap localities in Fig. 10 (see also Table 8). The HTC direction of six sills and dykes points upwards with a northwestern azimuth. One dyke (Viluy-8) has a downward southeastern azimuth direction (samples V158T3 and V163M2, Fig. 9). The reversal test has no statistical significance because there is only one normal direction out of 11 studied kimberlites and trap localities.

The HTC directions for traps and kimberlites are close to each other. We could not apply a fold test because most rocks have horizontal bedding. However, some sills have a small dip (5°–18°) that was measured in over- and underlying Ordovician sediments. The $k$ precision parameter is larger after tilt correction ($ks/kg=1.4$) but the fold test is statistically undetermined. This slight increase in the $k$-value may be seen as an indicator of the primary character of the HTC. In any case, the final direction does not change significantly before ($D=323.3°$, $I=-53.7°$, $k=22.4$, $\alpha_{95}=9.9°$) and after tilt correction ($D=319.1°$, $I=-49.3°$, $k=31.5$, $\alpha_{95}=8.3°$, $N=11$ localities; Fig. 10, Table 8). The Watson & Enkin (1993) fold test, based on 1000 trials, gives an optimum data grouping at 119.6 per cent unfolding, with 95 per cent confidence limits at 97.4 and 141.8 per cent. This is statistically indistinguishable from 100 per cent untilting and indicates that remanence is more probably pre-tilting. We regard the presence of two polarities as an additional factor in favour of a primary origin of the HTC, and thus prefer the tilt-corrected result. Additional support for this primary origin may come from the similarity of the HTC directions for different rock types (kimberlites and traps), and magnetic minerals (mainly titanomagnetite and magnetite). Another argument is the similarity in directions for sites located tens to hundreds of kilometres away from each other.

### *Kimberlites from the Mir and Sputnik pipes*

The 140 samples collected from 17 sites in the Late Devonian–Early Carboniferous Mir kimberlite pipe exhibit similar demagnetization characteristics (Fig. 12). Two components were isolated after thermal demagnetization. The first points northwards and down (NRM to 200 °C), while the HTC has a reversed

**Table 8.** Late Devonian–Early Carboniferous basalt flows and dyke mean directions of the high-temperature component of magnetization for the Markha and Viluy river traps (region around 63.5°N, 116.0°E) and kimberlite pipes of the Alakit–Markha region.

| Locality | *n* | *D*g (°) | *I*g (°) | *D*s (°) | *I*s (°) | *k* | $\alpha_{95}$ (°) | Notes |
|---|---|---|---|---|---|---|---|---|
| Markha 2, dyke | 12 samples | 293.7 | −49.9 | 293.7 | −49.9 | 23.7 | 9.6 | 2d + 10cc |
| Markha 4, sill | 16 samples | 326.2 | −42.6 | 326.2 | −42.6 | 28.8 | 7.0 | 16d |
| Markha 5, sill | 11 samples | 334.0 | −43.3 | 336.0 | −34.7 | 36.3 | 7.7 | 11d |
| Markha 6, sill | 9 samples | 324.7 | −56.3 | 330.3 | −48.3 | 21.2 | 11.4 | 9d |
| Viluy 6, sill | 10 samples | 352.7 | −65.9 | 321.9 | −57.7 | 54.2 | 6.6 | 10d |
| Viluy 7, dyke | 18 samples | 332.0 | −53.8 | 316.2 | −42.3 | 38.5 | 5.6 | 18d |
| Viluy 8, dyke | 13 samples | 201.9 | 69.4 | – | – | 147.7 | 3.4 | 13d |
| | | – | – | 154.2 | 68.0 | 142.7 | 3.5 | |
| Kimberlites from Sytikanskaya pipe | 9 sites | 298.1 | −60.1 | 298.1 | −60.7 | 27.0 | 10.1 | see Table 2 for details |
| Kimberlites from Yubileinaya pipe | 5 sites | 301.0 | −56.8 | 301.0 | −56.8 | 42.4 | 11.9 | see Table 4 for details |
| Kimberlites from Aikhal pipe | 21 samples | 318.9 | −33.9 | 318.1 | −33.9 | 9.0 | 11.2 | 15d + 6cc see Table 5 for details |
| Satellite body of Aikhal kimberlite pipe | 14 samples | 325.1 | −38.9 | 325.1 | −38.9 | 17.6 | 9.9 | 8d + 6cc see Table 6 for details |
| Mean | 11 localities | 323.3 | −53.7 | – | – | 22.4 | 9.9 | |
| | | – | – | 319.1 | −49.3 | 31.5 | 8.3 | |

Same abbreviations as in Table 5.

polarity. The LTC average direction ($D=318.3°$, $I=68.6°$, $k=67.0$, $\alpha_{95}=4.4°$, $N=17$ sites) does not coincide with the present geomagnetic field direction in the region ($D=353.1°$, $I=78.7°$), but is close to it. It is interpreted as a present-day or recent (up to Cenozoic) overprint (Fig. 12, Table 9). The mean HTC direction ($D=291.8°$, $I=-82.3°$, $k=16.4$, $\alpha_{95}=9.1°$, $N=17$ sites; Fig. 12, Table 9) is different from the other Palaeozoic kimberlite pipe directions. This has been interpreted as being the result of overprinting by the Late Permian–Early Triassic traps in the region (see next section). There are many

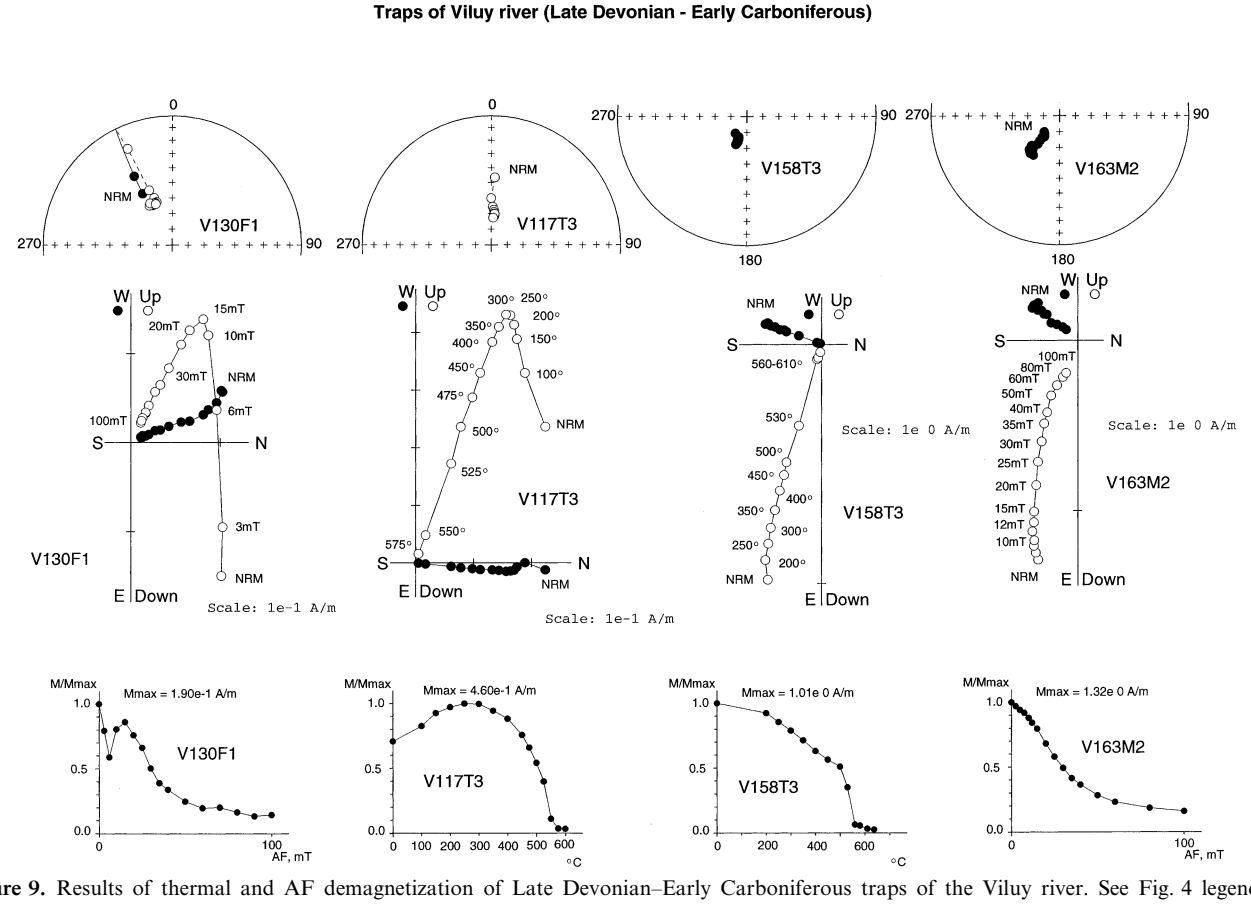


**Figure 9.** Results of thermal and AF demagnetization of Late Devonian–Early Carboniferous traps of the Viluy river. See Fig. 4 legend for further details.

**Table 9.** Site-mean palaeomagnetic directions for the low-, medium- and high-temperature components of magnetization of the Mir kimberlite pipe (62.5°N, 114.0°E).

| Site number | *n* | *D*g (°) | *I*g (°) | *D*s (°) | *I*s (°) | *k* | $\alpha_{95}$ (°) | Notes |
|---|---|---|---|---|---|---|---|---|
| Low-temperature component | | | | | | | | |
| MIR1 | 11 | 313.4 | 76.2 | | | 16.1 | 11.7 | 11d |
| MIR2 | 5 | 320.1 | 65.0 | | | 9.5 | 26.2 | 5d |
| MIR3 | 4 | 329.2 | 68.6 | | | 103.5 | 9.1 | 4d |
| MIR4 | 9 | 346.1 | 67.4 | | | 7.7 | 19.8 | 9d |
| MIR5 | 8 | 306.6 | 71.1 | | | 15.5 | 14.5 | 8d |
| MIR6 | 10 | 335.5 | 61.2 | | | 12.2 | 14.4 | 10d |
| MIR7 | 8 | 336.2 | 65.0 | | | 13.9 | 15.4 | 8d |
| MIR8 | 8 | 345.5 | 65.5 | | | 7.2 | 22.2 | 8d |
| MIR9 | 10 | 282.5 | 64.3 | | | 40.1 | 7.7 | 10d |
| MIR10 | 9 | 319.9 | 64.4 | | | 17.9 | 12.5 | 9d |
| MIR11 | 6 | 320.7 | 64.7 | | | 8.0 | 25.2 | 6d |
| MIR12 | 12 | 290.3 | 65.6 | | | 10.5 | 14.0 | 12d |
| MIR13 | 5 | 321.3 | 60.6 | | | 8.9 | 27.1 | 5d |
| MIR14 | 12 | 2.2 | 73.0 | | | 9.6 | 14.8 | 12d |
| MIR15 | 5 | 288.7 | 72.6 | | | 9.6 | 25.9 | 5d |
| MIR16 | 5 | 280.2 | 62.0 | | | 11.6 | 23.4 | 5d |
| MIR17 | 10 | 315.7 | 72.4 | | | 9.1 | 16.9 | 10d |
| Overall mean | 17 sites | 318.3 | 68.6 | – | – | 67.0 | 4.4 | |
| High-temperature component | | | | | | | | |
| MIR1 | 9 | 3.5 | −76.8 | – | – | 5.9 | 23.3 | 7d + 2cc |
| MIR2 | 6 | 354.6 | −76.2 | – | – | 27.9 | 14.4 | 2d + 4cc |
| MIR3 | 4 | 211.4 | −75.8 | – | – | 35.7 | 15.6 | 4d |
| MIR4 | 6 | 353.4 | −79.5 | – | – | 25.7 | 15.9 | 1d + 5cc |
| MIR5 | 5 | 281.0 | −45.8 | – | – | 12.1 | 25.8 | 2d + 3cc |
| MIR6 | 7 | 277.4 | −58.9 | – | – | 4.9 | 31.1 | 4d + 3cc |
| MIR7 | 6 | 260.6 | −70.7 | – | – | 11.5 | 24.1 | 1d + 5cc |
| MIR8 | 9 | 290.2 | −80.1 | – | – | 5.4 | 25.2 | 3d + 6cc |
| MIR9 | 7 | 80.9 | −68.3 | – | – | 28.6 | 12.6 | 2d + 5cc |
| MIR10 | 7 | 334.0 | −77.8 | – | – | 11.8 | 18.7 | 5d + 2cc |
| MIR11 | 5 | 138.4 | −80.8 | – | – | 29.0 | 15.5 | 3d + 2cc |
| MIR12 | 7 | 269.2 | −64.5 | – | – | 6.7 | 27.1 | 2d + 5cc |
| MIR13 | 8 | 55.9 | −88.0 | – | – | 4.7 | 28.7 | 7d + 1cc |
| MIR14 | 7 | 196.7 | −74.7 | – | – | 17.3 | 15.5 | 4d + 3cc |
| MIR15 | 4 | 139.7 | −70.0 | – | – | 49.3 | 14.0 | 3d + 1cc |
| MIR16 | 4 | 352.9 | −53.4 | – | – | 27.4 | 20.7 | 2d + 2cc |
| MIR17 | 9 | 251.8 | −77.7 | – | – | 10.7 | 17.3 | 3d + 6cc |
| Overall mean | 17 sites | 291.8 | −82.3 | – | – | 16.4 | 9.1 | |

Same abbreviations as in Table 5.

trap sills and dykes in the region, but there are no rock units above the top of the Mir pipe. This is probably due to erosion. The Jurassic conglomerates with kimberlite and trap material near the pipe confirm this interpretation.

*Kimberlites from the Sputnik pipe*

This pipe is located 5 km away from the Mir pipe. The results of NRM thermal demagnetization are shown in Fig. 13. The LTC is largely removed by 200–300 °C. The average direction at the sample level is $D = 12.8°$, $I = 71.3°$ ($k = 9.0$, $\alpha_{95} = 9.4°$, $N = 29$ samples; Fig. 13, Table 10). This direction does not coincide with but is close to the present geomagnetic field direction in the region and again reflects recent overprinting. The thermal demagnetization diagrams of the Mir and Sputnik samples are difficult to interpret. A large group of samples was not affected by the production of new magnetic minerals at high temperatures. Thus, the unblocking temperatures are between 200 and 300 °C and 500 and 550 °C. The HTC site-mean direction ($D = 309.9°$, $I = -70.7°$, $k = 28.5$, $\alpha_{95} = 12.8°$, $N = 10$ sites; Fig. 13, Table 10) is close to the HTC direction of the Mir pipe. We suggest that this component also results from overprinting by the Late Permian–Early Triassic traps. Two sites (Sp-2 and Sp-8) have low inclinations, which could affect some primary Palaeozoic directions. The large $\alpha_{95}$ values ($> 15°$) may be a consequence of mixing between Palaeozoic and Mesozoic directions at the different sites.

## Siberian traps of Late Permian–Early Triassic age

*Magnetic minerals*

Typical examples of IRM acquisition, thermomagnetic curves and hysteresis loops are shown in Fig. 14. IRM experiments indicate that saturation of the remanence corresponds to bulk coercivities around 0.25–0.3 T. The disappearance of magnetization occurs between 580 and 590 °C (possibly due to a slight miscalibration of temperatures), and the thermomagnetic

**Table 10.** Site-mean palaeomagnetic directions for the low- and high-temperature components of magnetization of the Sputnik kimberlite pipe (62.5°N, 114.0°E).

| Site number | *n* | *D*g (°) | *I*g (°) | *D*s (°) | *I*s (°) | *k* | $\alpha_{95}$ (°) | Notes |
|---|---|---|---|---|---|---|---|---|
| Low-temperature component | | | | | | | | |
| All sites | 29 samples | 12.8 | 71.3 | – | – | 9.0 | 9.4 | sample level |
| High-temperature component | | | | | | | | |
| Sp-1 | 6 | 297.4 | −63.2 | – | – | 10.9 | 22.0 | 4d + 2cc |
| Sp-2 | 7 | 298.3 | −54.2 | – | – | 5.6 | 28.7 | 4d + 3cc |
| Sp-3 | 13 | 303.2 | −67.6 | – | – | 1.8 | 38.5 | 2d + 11cc |
| Sp-4 | 7 | 307.3 | −71.1 | – | – | 29.9 | 12.4 | 4d + 3cc |
| Sp-5 | 6 | 229.9 | −66.3 | – | – | 5.1 | 33.7 | 4d + 2cc |
| Sp-6 | 7 | 286.2 | −80.2 | – | – | 13.9 | 16.8 | 7d |
| Sp-7 | 4 | 305.1 | −76.3 | – | – | 317.8 | 5.2 | 4d |
| Sp-8 | 7 | 332.2 | −45.3 | – | – | 15.1 | 16.2 | 6d + 1cc |
| Sp-9 | 6 | 280.8 | −82.1 | – | – | 37.3 | 11.3 | 5d + 1cc |
| Overall mean | 9 sites | 299.2 | −69.8 | – | – | 25.2 | 10.4 | all sites |
| Overall mean | 6 sites | 309.9 | −70.7 | – | – | 28.5 | 12.8 | only sites with $\alpha_{95} < 25°$ |

Same abbreviations as in Table 5.

curves are partly reversible. Hysteresis loops are compatible with single or pseudo-single domains. These observations suggest that magnetite dominates the remanence.

### *Traps around the Sytikanskaya kimberlite pipe*

10 sites have been sampled at this locality. Typical thermal demagnetization curves are shown in Fig. 15. An LTC with normal polarity (down and northwards) is observed below 250–300 °C. The corresponding site-mean direction was calculated for eight sites ($D = 305.7°$, $I = 68.2°$, $k = 168.1$, $\alpha_{95} = 4.3°$; Table 11), which presented a clear HTC component. The LTC direction does not coincide with the present-day geomagnetic field direction in the region ($D = 353.2°$, $I = 81.3°$). Between 300 and 500 °C the HTC component was easily isolated with reversal direction, $D = 273.3°$, $I = -64.1°$ ($k = 201.5$, $\alpha_{95} = 3.4°$, $N = 10$ sites; Fig. 15, Table 11).

**Table 11.** Site-mean palaeomagnetic directions for the low- and high-temperature components of magnetization of the Late Permian–Early Triassic basalt flow near the Sytikanskaya kimberlite pipe (66.11°N, 111.80°E).

| Site number | *n* | *D*g (°) | *I*g (°) | *D*s (°) | *I*s (°) | *k* | $\alpha_{95}$ (°) |
|---|---|---|---|---|---|---|---|
| Low-temperature component | | | | | | | |
| Stk-1 | 4 | 285.2 | 66.3 | – | – | 48.8 | 23.3 |
| Stk-2 | 5 | 279.4 | 65.0 | – | – | 9.5 | 26.2 |
| Stk-3 | 4 | 308.0 | 69.6 | – | – | 109.6 | 8.8 |
| Stk-4 | 4 | 313.5 | 68.8 | – | – | 326.9 | 5.1 |
| Stk-5 | 3 | 310.1 | 69.4 | – | – | 310.8 | 7.0 |
| Stk-6 | 3 | 318.6 | 67.6 | – | – | 575.9 | 5.1 |
| Stk-7 | 3 | 310.9 | 67.5 | – | – | 414.5 | 6.1 |
| Stk-8 | 4 | 322.8 | 66.2 | – | – | 95.3 | 9.5 |
| Overall mean | 8 sites | 305.7 | 68.2 | – | – | 168.1 | 4.3 |
| High-temperature component | | | | | | | |
| Stk-1 | 4 | 275.9 | −59.9 | – | – | 341.9 | 5.0 |
| Stk-2 | 5 | 262.6 | −67.0 | – | – | 126.3 | 6.8 |
| Stk-3 | 4 | 279.1 | −71.0 | – | – | 137.5 | 7.9 |
| Stk-4 | 5 | 278.7 | −61.8 | – | – | 50.1 | 10.9 |
| Stk-5 | 3 | 284.8 | −61.8 | – | – | 22.3 | 26.7 |
| Stk-6 | 3 | 277.6 | −64.5 | – | – | 467.5 | 5.7 |
| Stk-7 | 3 | 266.8 | −67.1 | – | – | 31.0 | 22.5 |
| Stk-8 | 4 | 266.5 | −59.4 | – | – | 40.0 | 14.7 |
| Stk-9 | 4 | 254.9 | −62.9 | – | – | 29.5 | 17.2 |
| Stk-10 | 4 | 285.1 | −62.7 | – | – | 51.3 | 12.9 |
| Overall mean | 10 sites | 273.3 | −64.1 | – | – | 201.5 | 3.4 |

Same abbreviations as in Table 5.

### *Traps around the Yubileinaya kimberlite pipe*

19 samples from four sites were demagnetized, and 16 yielded a well-defined LTC. The LTC direction (Fig. 16, Table 12) ($D = 334.8°$, $I = 64.1°$, $k = 22.9$, $\alpha_{95} = 7.9°$, $N = 16$ samples) is close to the present-day geomagnetic field and thus reflects a recent overprint. The overall mean direction of the HTC component is $D = 53.4°$, $I = 80.6°$ ($k = 635.1$, $\alpha_{95} = 3.6°$, $N = 4$ sites). In contrast to the traps from the Sytikanskaya pipe area traps, this sill has normal polarity. The direction is different from the reversed direction of the kimberlite pipes that were sampled a few hundred metres away from the trap sill. Thus we infer that the traps did not remagnetize all kimberlites. The

**Table 12.** Site-mean palaeomagnetic directions for the low- and high-temperature components of magnetization of the Late Permian–Early Triassic basalt flow near the Yubileinaya kimberlite pipe (66.0°N, 111.7°E).

| Site number | *n* | *D*g (°) | *I*g (°) | *D*s (°) | *I*s (°) | *k* | $\alpha_{95}$ (°) |
|---|---|---|---|---|---|---|---|
| Low-temperature component | | | | | | | |
| Overall mean | 16 samples | 334.8 | 64.1 | – | – | 22.9 | 7.9 |
| High-temperature component | | | | | | | |
| Yubil-1 | 5 | 74.8 | 80.0 | – | – | 78.0 | 8.7 |
| Yubil-2 | 5 | 38.5 | 80.5 | – | – | 114.3 | 7.2 |
| Yubil-3 | 5 | 58.9 | 78.7 | – | – | 54.4 | 10.5 |
| Yubil-4 | 4 | 37.3 | 81.7 | – | – | 77.4 | 10.5 |
| Overall mean | 4 sites | 53.4 | 80.6 | 53.4 | 80.6 | 635.1 | 3.6 |
| Overall mean | 19 samples | 54.1 | 80.5 | 54.1 | 80.5 | 81.6 | 3.7 |

Same abbreviations as in Table 5.

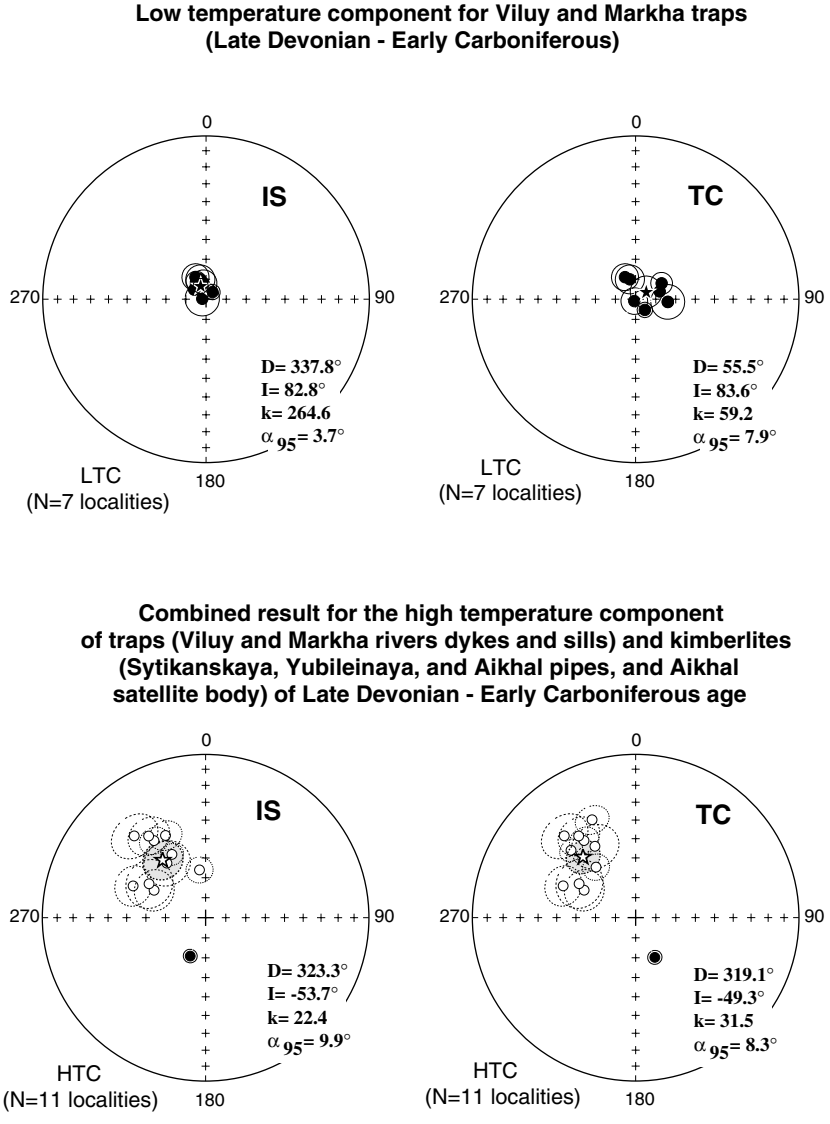


**Figure 10.** Equal-area projections of site-mean directions of LTC and HTC, with circles of 95 per cent confidence shown *in situ* (IS) and tilt-corrected (TC). Top: LTC for Viluy and Markha river dykes and sills; bottom: combined result of all Late Devonian-Early Carboniferous localities of the present study HTC for Viluy and Markha river dykes and sills and kimberlites from the Sytikanskaya, Yubileinaya, and Aikhal pipes and Aikhal satellite body. Other details as in Fig. 4.

sediments found in this region, at least those located a few hundred metres away from the traps, could therefore be expected to carry a primary magnetization. We also sampled some kimberlites 50 m away from the contact zone with the traps.

*Kimberlites of the Yubileinaya pipe (contact with traps)*

One or two components are present in the kimberlite samples that were taken between 1 and 50 m from the contact (Fig. 16). Evidence for a significant overprint linked to the emplacement of the traps was given by the absence of any clear HTC. In contrast, the LTC was clearly determined. Its average value, $D = 54.2^\circ$, $I = 72.3^\circ$ ($k = 25.0$, $\alpha_{95} = 12.3^\circ$, $N = 7$ sites; Table 13), coincides with the HTC direction of the traps.

**Table 13.** Site-mean palaeomagnetic directions for the low-temperature component of magnetization of the Late Devonian–Early Carboniferous kimberlites of the Yubileinaya pipe near the contact with a Late Permian–Early Triassic basalt flow (66.0°N, 111.7°E).

| Site number | *n* | *D*g (°) | *I*g (°) | *D*s (°) | *I*s (°) | *k* | $\alpha_{95}$ (°) |
|---|---|---|---|---|---|---|---|
| Yub-k-1 | 5 | 56.2 | 57.6 | – | – | 164.5 | 6.0 |
| Yub-k-2 | 6 | 62.2 | 52.8 | – | – | 377.1 | 3.5 |
| Yub-k-3 | 8 | 75.6 | 66.9 | – | – | 12.7 | 16.2 |
| Yub-k-4 | 3 | 6.7 | 69.6 | – | – | 60.3 | 16.0 |
| Yub-k-5 | 6 | 155.5 | 82.4 | – | – | 33.3 | 11.8 |
| Yub-k-6 | 7 | 2.9 | 85.1 | – | – | 52.0 | 8.4 |
| Yub-k-7 | 7 | 44.1 | 72.6 | – | – | 17.0 | 15.1 |
| Overall mean | 7 sites | 54.2 | 72.3 | – | – | 25.0 | 12.3 |

Same abbreviations as in Table 5.

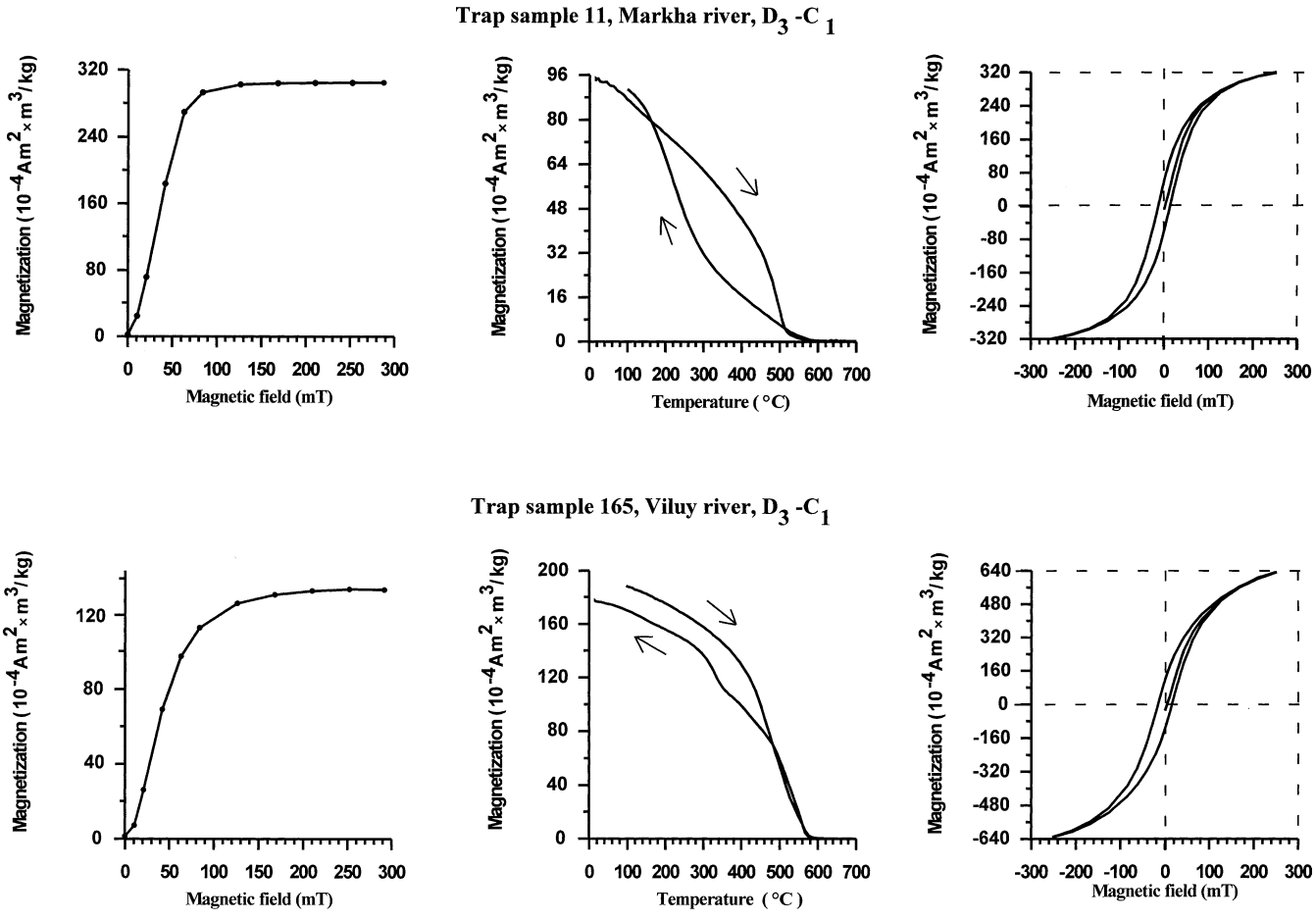


**Figure 11.** Results of rock magnetic experiments for Late Devonian–Early Carboniferous traps of the Markha and Viluy rivers. IRM acquisition curves (left), Curie point thermomagnetic curves $J_s$(T) (centre) and hysteresis loops (right).

*Traps around the Aikhal kimberlite pipe*

Typical thermal and AF demagnetization diagrams of samples from 10 sites taken in the Aikhal trap sill are shown in Fig. 17(a). The LTC is removed below 100–200 °C or 10 mT. Its average direction, $D=320.1°$, $I=78.7°$ ($k=89.1$, $\alpha_{95}=5.1°$; Fig. 17b, Table 14), indicates a present-day overprint. The mean direction of the HTC ($D=102.9°$, $I=81.9°$, $k=89.4$, $\alpha_{95}=5.1°$, $N=10$ sites; Fig. 17b, Table 14) has a normal polarity that is almost the same as for the traps near the Yubileinaya pipe. The differences between the Aikhal, Yubileynaya and Sytikanskaya trap directions are probably due to palaeosecular variation. The presence of two polarities is an additional indication for the primary origin of the remanence.

The mean directions of the HTCs of the three trap sills and the HTC of the Mir and Sputnik kimberlite pipes are shown in Fig. 17(c). The results are given in Table 15. The absence of metamorphism and other intrusions (except of Palaeozoic kimberlites and Permo-Triassic traps) in the area, the presence of two polarities for different sills and the overall good quality of the demagnetization diagrams strongly argue in favour of a primary magnetization for Permo-Triassic traps.

In contrast, the Mir and Sputnik kimberlites have been fully remagnetized. Indeed, their mean directions are extremely close to the Late Permian–Early Triassic trap directions. We checked further this hypothesis by sampling an additional trap sill of Palaeozoic age, which is cut by the Mir kimberlite pipe. The NRM intensities (0.3–0.6 mA $m^{-1}$) were 1000 times weaker than the intensities of the Viluy and Markha Palaeozoic traps. The LTC ($D=35.2°$, $I=70.7°$, $k=45.9$, $\alpha_{95}=11.4°$, $N=5$ samples) coincides with the present-day geomagnetic field, but the HTC could not be fully recovered. Its average direction was determined mainly from the great circles ($D=214.2°$, $I=-85.4°$, $k=14.9$, $\alpha_{95}=25.3°$, $N=5$ samples) and is close to the Permo-Triassic field.

Remagnetization of trap sills and the Mir and Sputnik kimberlite pipes was probably caused by extensive reheating related to the Permo-Triassic trap intrusions, which can be observed a few tens of kilometres away and were most probably eroded near the Mir pipe.

We calculated an average direction for all five localities: the Mir and Sputnik pipes and the Sytikanskaya, Yubileinaya and Aikhal pipe trap sills (Fig. 17c, Table 15). The reversal test is positive at the 95 per cent level (critical $\gamma=20°$ and angle between two averages 11°; McFadden & Lowes 1981). The presence of two polarities has already been demonstrated in Permo-Triassic traps from the western part of the Siberian platform (Lind *et al.* 1994; Gurevitch *et al.* 1995; Westphal *et al.* 1998). This observation is now valid also for the remote eastern part of the traps.

**Table 14.** Site-mean palaeomagnetic directions for the low- and high-temperature components of magnetization of the Late Permian–Early Triassic basalt flow of the Aikhal kimberlite pipe (66.17°N, 111.33°E).

| Site number | *n* | *D*g (°) | *I*g (°) | *D*s (°) | *I*s (°) | *k* | $\alpha_{95}$ (°) |
|---|---|---|---|---|---|---|---|
| Low-temperature component | | | | | | | |
| Aikh-1 | 6 | 7.0 | 80.7 | – | – | 214.5 | 4.6 |
| Aikh-2 | 5 | 328.9 | 72.5 | – | – | 115.4 | 7.2 |
| Aikh-3 | 6 | 336.5 | 80.5 | – | – | 78.2 | 7.6 |
| Aikh-4 | 6 | 334.7 | 78.1 | – | – | 182.5 | 5.0 |
| Aikh-5 | 6 | 345.5 | 76.1 | – | – | 44.5 | 10.1 |
| Aikh-6 | 4 | 298.8 | 77.6 | – | – | 51.0 | 13.0 |
| Aikh-7 | 6 | 281.0 | 83.0 | – | – | 82.6 | 7.4 |
| Aikh-8 | 4 | 318.0 | 84.3 | – | – | 177.0 | 6.9 |
| Aikh-9 | 7 | 295.0 | 61.0 | – | – | 10.7 | 19.4 |
| Aikh-10 | 2 | 319.4 | 83.0 | – | – | – | – |
| Overall mean | 10 sites | 320.1 | 78.7 | – | – | 89.1 | 5.1 |
| High temperature component | | | | | | | |
| Aikh-1 | 6 | 43.5 | 81.5 | – | – | 24.7 | 13.7 |
| Aikh-2 | 6 | 22.0 | 89.2 | – | – | 39.7 | 10.8 |
| Aikh-3 | 4 | 116.0 | 72.8 | – | – | 51.4 | 12.9 |
| Aikh-4 | 6 | 30.4 | 87.2 | – | – | 340.9 | 3.6 |
| Aikh-5 | 6 | 85.0 | 76.4 | – | – | 682.9 | 2.6 |
| Aikh-6 | 5 | 155.0 | 83.7 | – | – | 27.2 | 14.9 |
| Aikh-7 | 6 | 134.5 | 79.6 | – | – | 76.4 | 7.7 |
| Aikh-8 | 7 | 129.9 | 71.7 | – | – | 22.2 | 13.1 |
| Aikh-9 | 8 | 98.4 | 86.4 | – | – | 256.2 | 3.5 |
| Aikh-10 | 6 | 78.2 | 72.6 | – | – | 61.1 | 8.6 |
| Overall mean | 10 sites | 102.9 | 81.6 | – | – | 89.4 | 5.1 |

Same abbreviations as in Table 5.

## DISCUSSION

### Palaeomagnetic poles from Late Devonian–Early Carboniferous kimberlites and traps

We have shown that two magnetization components could be separated in all 16 localities that have been studied. In most cases, although not all, the LTC could be interpreted as either a present or a Cenozoic geomagnetic field overprint, or the resultant of several remagnetizations. Below we discuss the palaeomagnetic poles derived from the HTCs.

The individual palaeomagnetic poles for the Viluy and Markha river traps, the Yubileinaya and Aikhal kimberlite pipes, the satellite dyke of the Aikhal pipe and the Sytikanskaya kimberlite pipe are summarized in Table 16. At this stage we cannot constrain the exact age of the rocks at these localities. Table 17 gives a selection of palaeomagnetic poles of Late Devonian–Early Carboniferous age for the Siberian platform (Fig. 18). The data found in palaeomagnetic databases are very scattered. Many poles published before 1980 have low reliability (e.g. code of laboratory testing; McElhinny & Lock 1996). There is often a unique AF demagnetization step or no information regarding the demagnetization procedure. Many studies include viscosity tests but do not indicate the presence of demagnetization. Many poles do not include any description. Therefore many poles (i.e. those from the Russian database) must be regarded with great caution. However, these are often the only available data for Siberia.

Smethurst *et al.* (1998) selected poles based on the geological ages of the formations. Unfortunately none of these poles was ever published in refereed journals and there is no indication about the techniques used to extract the primary magnetization. The present study has shown that overprints are frequently resistant to AF peak fields as high as 25 mT and thus not removed by 8 mT demagnetizations, which were used frequently in the 1970s. Similar remarks would be valid for many dates published during the same period. This can be illustrated by comparing the K–Ar dating of West Siberian traps prior to 1990 with the most resent Ar–Ar ages (Almukhamedov & Zolotukhin 1989; Renne *et al.* 1995; Venkatesan *et al.* 1997). Note also that the paper by Zhitkov *et al.* (1994), which two of us (VAK and KMK) coauthored, was a preliminary study, in order to determine which type of kimberlite would be appropriate for palaeomagnetism. The differences between the directions published by Zhitkov *et al.* (1994) and the present results are due to measurements of a much larger number of samples.

In Fig. 18(a) we plot the palaeomagnetic poles obtained in this study that are listed in Table 16. The average pole position (11.1°N, 149.7°E, $A_{95}=8.9°$) for the Late Devonian–Early Carboniferous kimberlites and traps shown by a star in Fig. 18 is quite distinct from the coeval poles selected in Smethurst *et al.* (1998) to constrain the Siberian APWP at 360–380 Ma. We cannot define the age interval better than 377–350 Ma. Fig. 18(b) shows all poles from Table 17. The large scatter inherent to the published poles can thus be seen as a consequence of their poor reliability and partly also of age uncertainties.

### Palaeomagnetic poles from Late Permian–Early Triassic traps

All reliable poles for the Late Permian–Early Triassic traps of Siberia have been summarized in Table 18. Table 19 gives all poles related to these periods from the McElhinny & Lock

**Table 15.** Late Permian–Early Triassic basalt flow and kimberlite pipe mean directions of the high-temperature component of magnetization.

| Locality | *n* | *D*g (°) | *I*g (°) | *D*s (°) | *I*s (°) | *k* | $\alpha_{95}$ (°) | Notes |
|---|---|---|---|---|---|---|---|---|
| Kimberlites from Mir pipe | 17 | 291.8 | −82.3 | – | – | 16.4 | 9.1 | remagnetization |
| Kimberlites from Sputnik pipe | 6 | 309.9 | −70.7 | – | – | 28.5 | 12.8 | remagnetization |
| Traps of kimberlite pipe Sytikanskaya | 10 | 273.3 | −64.1 | – | – | 201.5 | 3.4 | primary magnetization |
| Traps of kimberlite pipe Yubileinaya | 4 | 53.4 | 80.6 | – | – | 635.1 | 3.6 | primary magnetization |
| Traps of kimberlite pipe Aikhal | 10 | 102.9 | 81.6 | – | – | 89.4 | 5.1 | primary magnetization |
| Overall mean | 5 localities | 101.5 | 77.0 | – | – | 63.1 | 9.7 | |

Same abbreviations as in Table 5.

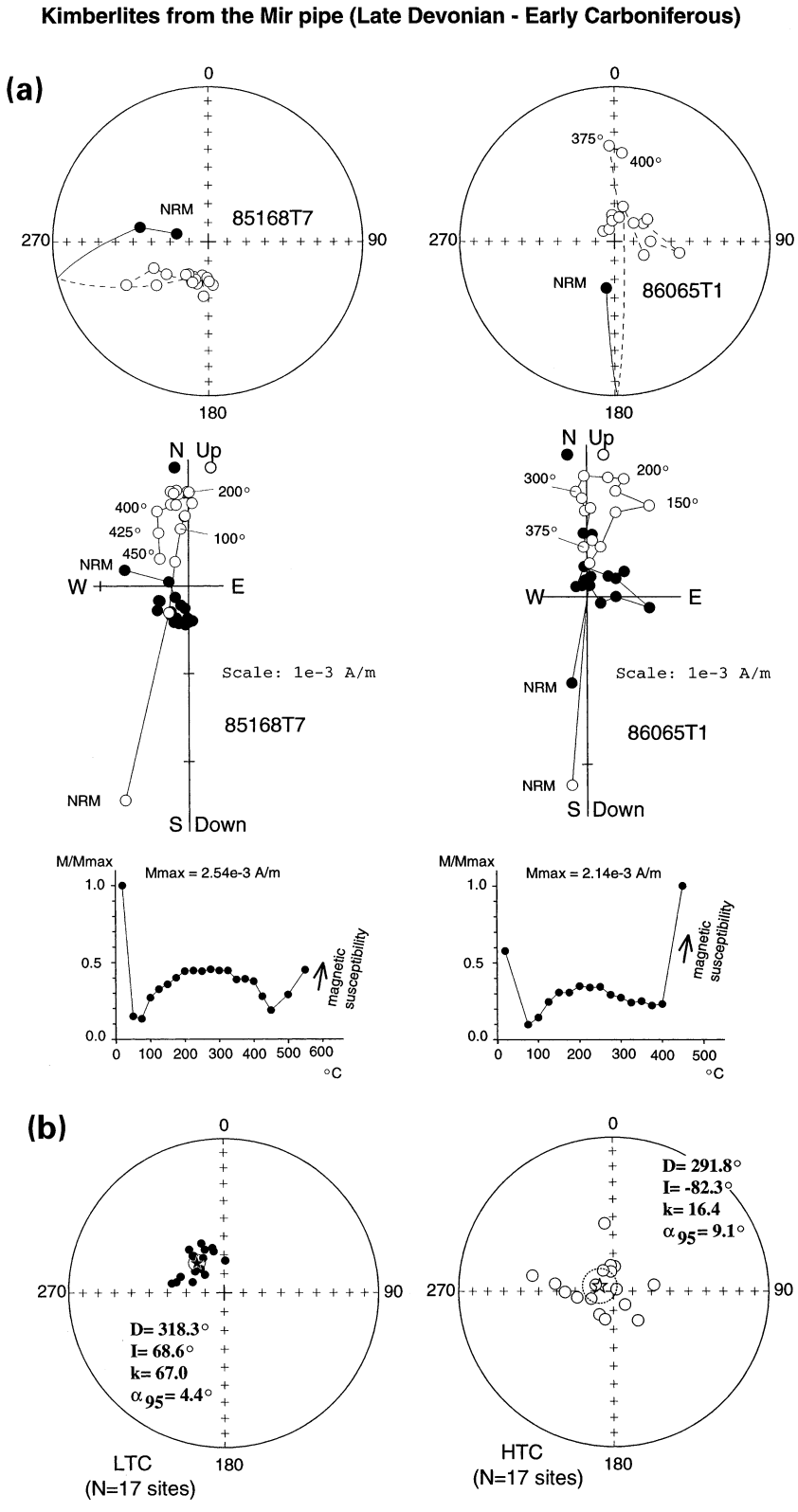


**Figure 12.** (a) Results of thermal demagnetization of Late Devonian–Early Carboniferous kimberlite samples of the Mir pipe. Arrows near magnetic intensity decay curves show increasing magnetic susceptibility. (b) Equal-area projections of site-mean directions of LTC and HTC, with circles of 95 per cent confidence. All shown *in situ*. Other details as in Fig. 4.

(1996) database. Many poles cannot be considered as reliable. The most reliable poles from Pisarevsky (1982) have no multicomponent analysis and were not published in a refereed journal. The pole given by Zhitkov *et al.* (1994) was defined from preliminary directions. The palaeomagnetic pole of Solodovnikov (1994) seems to be acceptable, but the paper deals with palaeointensity and does not incorporate enough experimental information to be fully acceptable. However, it

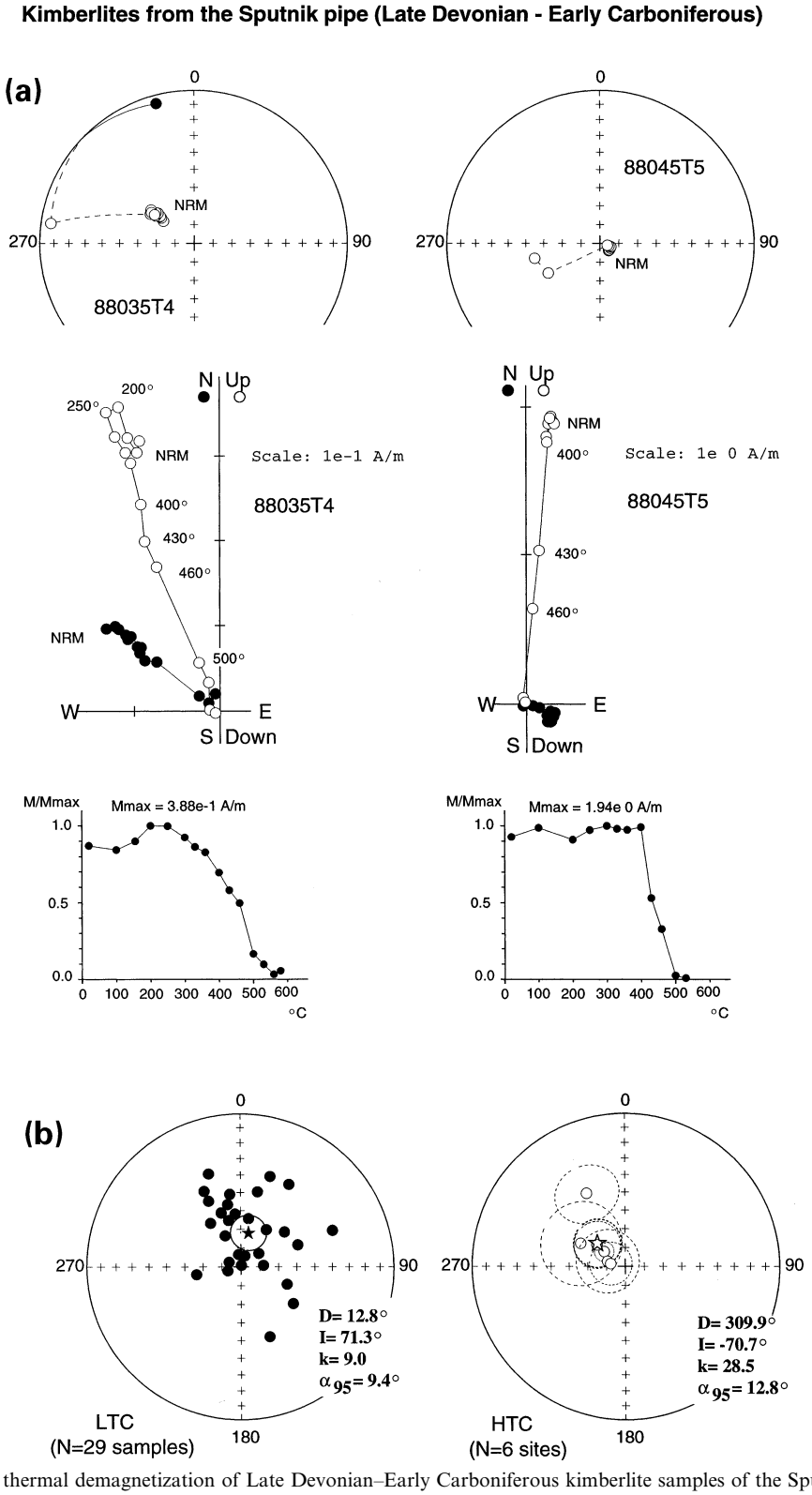


**Figure 13.** (a) Results of thermal demagnetization of Late Devonian–Early Carboniferous kimberlite samples of the Sputnik pipe. (b) Equal-area projections of site-mean directions of LTC and HTC, with circles of 95 per cent confidence. All shown *in situ*. Other details as in Fig. 4.

includes a large number of samples with two polarities, and the overall mean direction coincides with the present results.

Two special palaeomagnetic reports were published by Lind *et al.* (1994) and Gurevitch *et al.* (1995) in international journals for the Late Permian–Early Triassic traps. These studies are listed in Table 18. Our results of the Late Permian–Early Triassic traps, which cover the Yubileinaya, Aikhal and Sytikanskaya kimberlite pipes, were combined with the overprinted poles of the Mir and Sputnik kimberlite pipes (poles 1–5 in Table 18) and with the western Taimyr traps poles (poles 6–9

**Table 16.** Late Devonian–Early Carboniferous palaeomagnetic poles from the present study.

| Pole | Formation | Age (Ma) | Site | | Palaeopole | | *dp*/*dm* ($A_{95}$) | *N* | Palaeolat |
|---|---|---|---|---|---|---|---|---|---|
| | | | Lat | Lon | Lat | Lon | | | |
| 1 | Kimberlites from Sytikanskaya pipe | 377–350 | 66.11 | 111.8 | 27.8 | 159.9 | 11.8/15.4 | 9S | 41.7±11.8 |
| 2 | Kimberlites from Yubileinaya pipe | 377–350 | 66.0 | 111.7 | 22.8 | 159.4 | 12.5/17.3 | 5S | 37.4±12.5 |
| 3 | Kimberlites from Aikhal pipe | 377–350 | 66.17 | 111.33 | 0.2 | 149.9 | 7.3/12.8 | 21 s | 18.6±7.3 |
| 4 | Satellite body of Aikhal kimberlite pipe area | 377–350 | 66.17 | 111.33 | 2.0 | 143.4 | 7.0/11.8 | 14 s | 22.0±7.0 |
| 5 | Markha −2, trap dyke | 377–350 | 64.95 | 116.55 | 18.4 | 172.6 | 8.6/12.8 | 12 s | 30.7±8.6 |
| 6 | Markha −4, trap sill | 377–350 | 64.65 | 116.62 | 3.1 | 147.0 | 5.3/8.6 | 16 s | 24.7±5.3 |
| 7 | Markha −5, trap sill | 377–350 | 64.53 | 116.63 | −4.4 | 139.3 | 5.1/8.9 | 11 s | 19.1±5.1 |
| 8 | Markha −6, trap sill | 377–350 | 64.55 | 116.63 | 6.7 | 142.4 | 9.8/14.9 | 9 s | 29.3±9.8 |
| 9 | Vilui−6, trap sill | 377–350 | 62.32 | 116.03 | 15.2 | 146.1 | 7.1/9.7 | 10 s | 38.3±7.1 |
| 10 | Vilui−7, trap dyke | 377–350 | 62.30 | 116.06 | 3.5 | 155.2 | 4.2/6.9 | 18 s | 24.5±4.2 |
| 11 | Vilui−8, trap dyke | 377–350 | 62.30 | 116.06 | 25.2 | 133.7 | 4.9/5.9 | 13 s | 51.1±4.9 |
| | Mean pole | 377–350* | 64.6 | 114.7 | 11.1 | 149.7 | 8.9 | 11 L | 31.2±8.9 |

Lat (Lon): latitude (longitude) of sampling sites or palaeomagnetic poles; $A_{95}$: radius of the 95 per cent confidence circle of the virtual palaeomagnetic pole; *dp*/*dm*: semi-axes of the confidence circle of the palaeomagnetic pole; Palaeolat.: palaeolatitude; *N*: number of localities (L), samples (s) or sites (S) used to determine pole.

* Corresponding geological age is Frasnian–Tournaisian

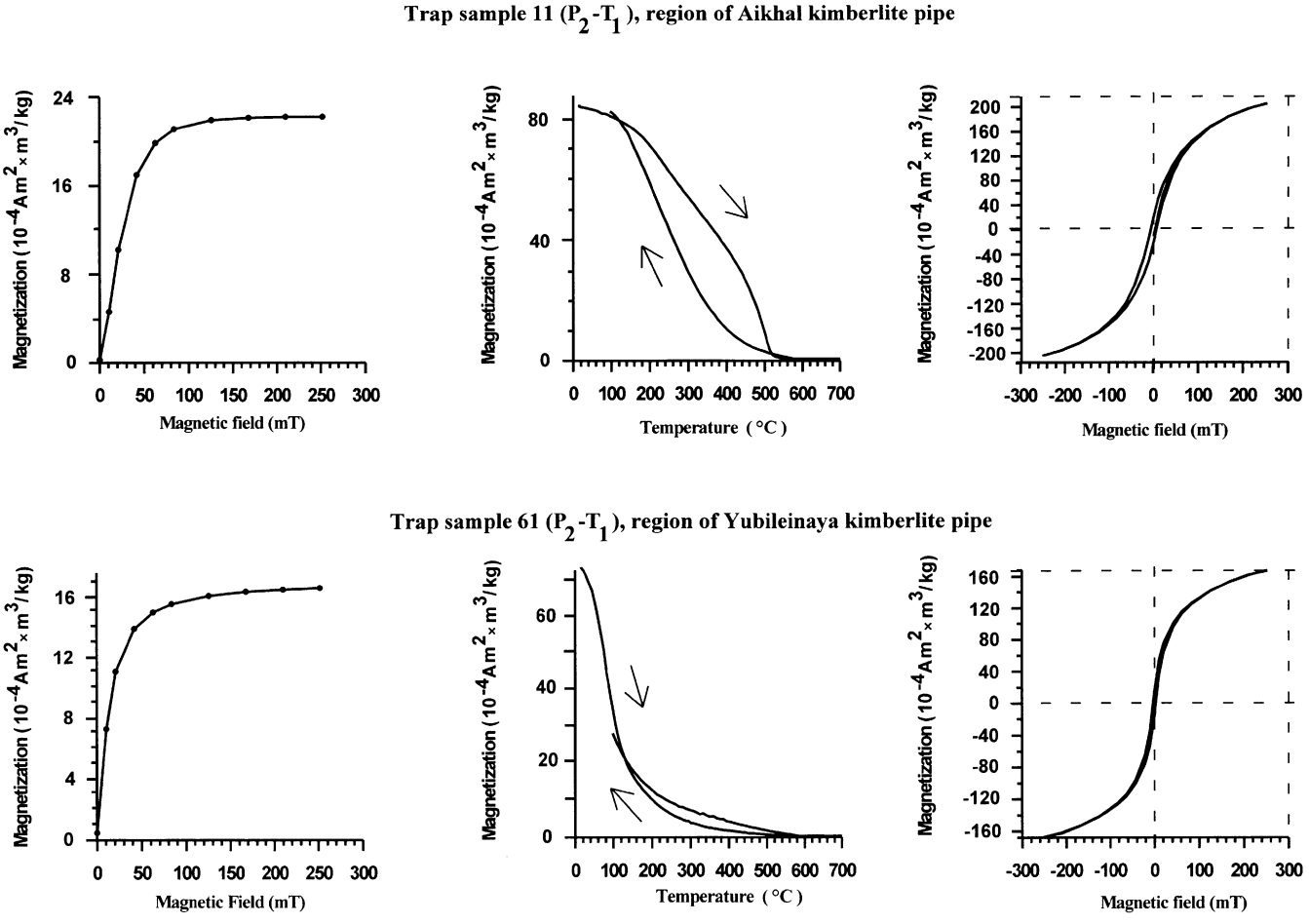


**Figure 14.** Results of rock magnetic experiments for Late Permian–Early Triassic traps of the Alakit–Markha region (region of Late Devonian–Early Carboniferous Sytikanskaya, Yubileinaya and Aikhal kimberlite pipes). IRM acquisition curves (left), Curie point thermomagnetic curves $J_s$(T) (centre) and hysteresis loops (right).

**Table 17.** Late Devonian–Early Carboniferous selected palaeomagnetic poles for the Siberian platform.

| | Rock unit | RLat | RLong | Code | Low mag. age | High mag. age | Dec | Inc | $N$ | $k$ | $\alpha_{95}$ | PLat | PLong | $dp/dm$ | Reference |
|---|---|---|---|---|---|---|---|---|---|---|---|---|---|---|---|
| 1 | River Angara basin sills | 56 | 101 | 2 (A) | 290 | 363 | 286 | −68 | 127 | 33 | 2 | 33 | 147 | 2.8/3.4 | Davydov & Kravchinsky (1971) |
| 2 | Angara River intrusions and sediments | 55 | 101 | 2 (40 mT) | 290 | 363 | 95 | 49 | 673 | 56 | 1 | 21 | 170 | 0.9/1.3 | Davydov & Kravchinsky (1973) |
| 3 | Aldan Region porphyries | 59 | 125.5 | 2 (A) | 290 | 363 | 142 | 67 | 28 | 67 | 6 | 23 | 151 | 8.2/9.9 | Kamysheva (1973) |
| 4 | Angara River intrusions and sediments | 55 | 99 | 2 (A) | 290 | 363 | 117 | 76 | 30 | 38 | 3 | 37 | 130 | 5.1/5.5 | Davydov & Kravchinsky (1973) |
| 5 | Tushaminsk Group | 58.5 | 102.5 | 2 (20 mT) | 303 | 323 | 307 | −85 | 34 | 22 | 5 | 51 | 118 | 9.8/9.9 | Davydov & Kravchinsky (1971) |
| 6* | Ygyattin Series | 63.5 | 115.6 | 2 (8 mT) | 323 | 377 | 205 | 45 | 20 | 22 | 7 | 3 | 93 | 6/9 | Kamysheva (1975) |
| 7 | Lena River sediments | 72.3 | 126.9 | 2 (TA) | 323 | 363 | 21 | −70 | 82 | 38 | 25 | 38 | 112 | 37/43 | Pisarevsky (1982) |
| 8 | Yubileinaya kimberlite pipe | 66 | 111.7 | 3 (T) | 323 | 377 | 323.8 | −63 | 37 | 100.2 | 4.2 | −23.8 | 319.2 | 5.0/6.4 | Zhitkov *et al.* (1994) |
| 9 | Ygyattin Series, Kutchugunursk Group | 63.5 | 116.5 | 2 (AV) | 332 (K–Ar | 352 342) | 183 | 61 | 84 | 17 | 17 | 16 | 115 | 19.9/26 | Kamysheva (1973) |
| 10 | Minusa tuffs and sediments | 53 | 91 | 2 (AT) | 333 | 363 | 314 | −47 | 17 | 9 | 12 | 1 | 131 | 10/15.5 | Aparin (1973) |
| 11 | Sytykanskaya kimberlite pipe | 66.1 | 111.8 | 3 (T) | 340 | 348 | 322.4 | −64 | 60 | 42 | 5.8 | −25.2 | 320 | 7.3/9.2 | Zhitkov *et al.* (1994) |
| 12 | Olenek Region Intrusions | 70.3 | 119.5 | 2 (A) | 345 | 375 | 195 | 68 | 24 | 23 | 6 | 32 | 109 | 8/10 | Kamysheva (1975) |
| 13 | Olenek Region Intrusives | 70.4 | 120.4 | 2 (A) | 345 | 375 | 164 | 75 | 93 | 75 | 11 | 43 | 130 | 18.3/20.1 | Kamysheva (1973) |
| 14 | Nadaltai, Altai, Bistryan and Tuba Groups | 54 | 91 | 2 (TA) | 349 | 367 | 299 | −70 | 114 | 44 | 4 | 29 | 127 | 5.9/6.9 | Aparin (1973) |
| 15 | Taidon Horizon | 68 | 89 | 2 (TAV) | 350 | 354 | 107 | 64 | 14 | 33 | 7 | 36 | 145 | 8.9/11.2 | Goncharov (1973) |
| 16 | Ygyattin Dolerites | 63.9 | 115.3 | 2 (A) | 358 (K–Ar | 376 367 ± 9) | 192 | 73 | 17 | 19 | 8 | 33 | 108 | 13/14 | Kamysheva (1975) |
| 17* | Ygyalta Series volcanics and intrusives | 63.7 | 116.5 | 2 (A) | 363 5 (K–Ar | 391 374) | 173 | 58 | 66 | 13 | 5 | 13 | 122 | 6/8 | Kamysheva (1975) |
| 18 | River Yenisei redbeds | 56 | 93 | 2 (20 mT) | 363 | 377 | 301 | −60 | 18 | 6 | 16 | 19 | 136 | 18.3/24.2 | Davydov & Kravchinsky (1971) |
| 19 | Ygyalta Series | 62.6 | 115.6 | 2 (10.5 mT, 30 days) | 363 | 377 | 227 | 80 | 18 | 42 | 5 | 46 | 93 | 9/10 | Kamysheva (1975) |
| 20 | Kalargon and Foka Groups | 69 | 88 | 2 (AT) | 363 | 377 | 89 | 77 | 112 | 16 | 3 | 58 | 141 | 5.2/5.6 | Lind (1973) |
| 21 | Olenek Region intrusives | 70.5 | 120.5 | 2(15 mT, 30 days) | 363 | 417 | 17 | −47 | 26 | 18 | 7 | 9 | 105 | 5.8/9 | Kamysheva (1973) |
| 22 | Oidanovo Group | 56 | 93 | 2 | 367 | 377 | 149 | −6 | 13 | 9 | 13 | −31 | 130 | 6/13 | Rodionov & Komissarova (1975) |
| 23 | Kokhai and Oidanovo Groups | 53 | 91 | 2 (TA) | 367 | 377 | 294 | −72 | 30 | 10 | 10 | 33 | 127 | 15.5/17.6 | Aparin (1973) |
| 24* | Fergana volcanics and sediments | 72.4 | 127 | 2 (TAV) | 367 | 377 | 31 | −66 | 16 | 21 | 8 | 32 | 104 | 11/13 | Pisarevsky (1982) |
| 25 | Oidanovo, Kokhai and Tuba Groups | 53 | 90 | 2 (40 mT) | 367 | 377 | 114 | 7 | 36 | 4 | 14 | −11 | 158 | 7/14 | Rodionov & Komissarova (1975) |

RLat, RLong: latitude, longitude of the sampling locality; Code: laboratory analytical procedures code from database of McElhinny & Lock (1996), laboratory treatment shown as thermal (T), alternating field (A), and viscous demagnetizations (V); *Low mag. age*, *High mag. age*: low, high limits of the magnetization age in Ma; Dec, Inc: Declination, Inclination of the primary magnetization vector; N: number of samples or sites in the study; $k$, $\alpha_{95}$—precision parameter and half angle radius of the 95 per cent probability confidence cone; Plat, Plong: latitude, longitude of the palaeomagnetic pole; $dp/dm$: semi-axes of the 95 per cent confidence ellipse of paleomagnetic pole.

*Poles used by Smethurst *et al.* (1998) for Siberian APWP.

**Table 18.** Late Permian–Early Triassic palaeomagnetic poles from the present study and selected poles from Siberia.

| Pole | Formation | Age of studied component (Ma) | Site | | Palaeopole | | *dp*/*dm* ($A_{95}$) | *N* | Palaeolat. | Reference |
|---|---|---|---|---|---|---|---|---|---|---|
| | | | Lat | Lon | Lat | Lon | | | | |
| 1 | Kimberlites from Mir pipe (overprint component) | 250±1.6 | 62.5 | 114.0 | 54.2 | 138.5 | 17.3/17.7 | 17S | 74.9±17.3 | This study |
| 2 | Kimberlites from Sputnik pipe (overprint component) | 250±1.6 | 62.5 | 114.0 | 33.8 | 146 | 19.3/22.2 | 6S | 55.0±19.3 | This study |
| 3 | Traps near Sytikanskaya kimberlite pipe | 250±1.6 | 66.11 | 111.8 | 39.8 | 176.6 | 4.3/5.4 | 10S | 45.8±4.3 | This study |
| 4 | Traps near Yubileinaya kimberlite pipe | 250±1.6 | 66.0 | 111.7 | 71.7 | 161.3 | 6.7/6.9 | 4S | 71.7±6.7 | This study |
| 5 | Traps near Aikhal kimberlite pipe | 250±1.6 | 66.17 | 111.33 | 58.4 | 143.1 | 9.6/9.9 | 10S | 73.5±9.6 | This study |
| 6 | Wesren Taimyr traps | 250±1.6 | 72.9 | 84.0 | 59.0 | 150.0 | 17/18 | 29 s | 61.7±17.0 | Gurevitch *et al.* (1995) |
| 7 | Noril'sk area traps (reverse polarity, AF treatment) | 250±1.6 | 69.5 | 89.5 | 38.0 | 145.0 | 23.0 | 10 s | 47.1±23.0 | Lind *et al.* (1994) |
| 8 | Noril'sk area traps (normal polarity, AF treatment) | 250±1.6 | 69.5 | 89.5 | 43.0 | 144.0 | 10.6 | 35 s | 52.0±10.6 | Lind *et al.* (1994) |
| 9 | Noril'sk area traps (normal polarity, thermal treatment) | 250±1.6 | 69.5 | 89.5 | 54.0 | 144.0 | 15.0 | 90 s | 61.3±15.0 | Lind *et al.* (1994) |
| | Mean pole | 250±1.6* | 64.60 | 114.7 | 50.8 | 149.6 | 9.4 | 9 L | 67.3±9.4 | |

Lat (Lon): latitude (longitude) of sampling sites or palaeomagnetic poles; $A_{95}$: radius of the 95 per cent confidence circle of the virtual palaeomagnetic pole; *dp*/*dm*: semi-axes of the confidence circle of the palaeomagnetic pole; *N*: number of localities (L), samples (s) or sites (S) used to determine pole; Palaeolat.: palaeolatitude.

* This age is based on geochronology (Renne & Basu 1991; Campbell *et al.* 1992; Renne *et al.* 1995; Venkatesan *et al.* 1997).

in Table 18) in order to calculate an average palaeomagnetic pole for the Permo-Triassic traps. This pole position (50.8°N, 149.6°E, $A_{95}=9.4°$), shown in Fig. 19(a), is close to the 248 Ma pole position proposed by Smethurst *et al.* (1998). The results are in good agreement with Hofmann (1997) and Westphal *et al.* (1998), who reported the presence of two polarities and palaeolatitudes from 64.5° to 71.7° from the study of a long core in an Early Triassic section of west Siberia.

## Palaeopositions of the Siberian platform in the Late Devonian and Early Triassic

Based on our new palaeomagnetic poles, we propose palaeoreconstructions of the Siberian platform and some related blocks for the Late Devonian–Early Carboniferous traps and kimberlites (360 Ma) and Late Permian–Early Triassic traps (250 Ma) (Fig. 20). The reconstruction of the Siberian platform has been made according to these new pole positions. We used the Mongol–Okhotsk suture as the southern border of the Siberian platform. It is now generally accepted that the Mongol–Okhotsk ocean, lying between Siberia to the north (in present-day coordinates) and Amuria/North China to the south, was closed between the Late Permian in Eastern Mongolia, the Jurassic in Trans-Baikalia and the Cretaceous in the Pacific part of Russia (Kuzmin & Fillipova 1978; Parfenov 1984; Kravchinsky 1990; Zonenshain *et al.* 1990; Zhao *et al.* 1990; Enkin *et al.* 1992; Gusev & Khain 1995; Xu *et al.* 1997; Halim *et al.* 1998a; Kravchinsky *et al.* 2001). Reconstruction of the North China platform relies on data from Zhao *et al.* (1996), Gilder *et al.* (1996) and Gilder & Courtillot (1997), and the palaeoposition of the Amuria block follows Zhao *et al.* (1996) and Kravchinsky *et al.* (2001). In order to constrain the palaeoposition of the Siberian platform, we used the APWP of Siberia from Smethurst *et al.* (1998) at 435 Ma as only available data compilation for that age, and the present data set for 360 and 250 Ma.

The palaeolatitude and rotational changes of the Siberian platform are shown in Fig. 20 (top). Prior to 360 Ma, the Russian platform (with Baltica and the Avalonian part of Western Europe) had already been amalgamated with Laurussia (Laurentia and Russia) (Smethurst *et al.* 1998). The 435 Ma reconstruction follows Smethurst *et al.* (1998). The 360 Ma reconstruction is based on results obtained in the present study. As far as the 435 Ma result can be trusted, it appears that Siberia did not change latitude significantly, but rotated clockwise by some 60° between 450 and 360 Ma. There are unfortunately no reliable palaeomagnetic data for Siberia between 360 and 250 Ma. A Late Permian pole from the Alentuy suite in Trans-Baikalia (Kravchinsky *et al.* 2001) provides a unique palaeolatitudinal control (63.8°N±13.8°), which is consistent with the present study. Northward motion of Siberia to high northern latitudes was associated with a ~60° clockwise rotation between 360 and 250 Ma.

Zhao *et al.* (1996, following Van der Voo 1993 and Li *et al.* 1993) showed that North China was at the equator in the Middle Devonian. At this time Tarim was close to subequatorial, with some northward motion (Bai *et al.* 1987; Li *et al.* 1990). No palaeomagnetic data have been obtained from Inner Mongolia (Amuria block) for early middle Palaeozoic times. The position of the Russian platform (with Baltica) is reconstructed after Smethurst & Khramov (1992). Kazakhstan is positioned according to Pechersky & Didenko (1995). Using single-zircon stepwise evaporation $^{207}Pb/^{206}Pb$ and whole-rock Rb–Sr methods, Montero *et al.* (2000) have dated the main facies of four Variscan batholiths of the Urals from different geodynamic environments. Their data indicate that the age of cessation of movements along the Main Uralian Fault and the transition from subduction to continent–continent collision

**Table 19.** Late Permian–Early Triassic selected palaeomagnetic poles for the Siberian platform.

| | Rock unit | RLat | RLong | Code | Low mag. age | High mag. age | Dec | Inc | $N$ | $k$ | $\alpha_{95}$ | PLat | PLong | $dp/dm$ | Reference |
|---|---|---|---|---|---|---|---|---|---|---|---|---|---|---|---|
| 1 | Lena River sediments | 72.6 | 124.7 | 2 (350 °C, 35–60 mT) | 178 | 241 | 174 | 76 | 26 | 210 | 9 | 47 | 129 | 4/16 | Pisarevsky (1982) |
| 2 | Anabar-Udzha region intrusives | 71.4 | 115.2 | 2 (10 mT) | 208 | 245 | 124 | 73 | 121 | 28 | 10 | 46 | 153 | 15.9/17.8 | Kamysheva (1971) |
| 3 | Alamdzhan region intrusives | 63.6 | 112.1 | 2 (10–15 mT) | 208 | 245 | 100 | 76 | 284 | 700 | 2 | 51 | 155 | 3.4/3.7 | Kamysheva (1971) |
| 4 | Mid Vilyui region tuffs | 63.5 | 111.5 | 2 (A) | 241 | 245 | 289 | −56 | 26 | 45 | 4 | 25 | 168 | 4.1/5.7 | Kamysheva (1973) |
| 5 | Syverminskaya–Mokulaevskaya Suites | 69.5 | 91 | 3 (T) | 241 | 245 | 100 | 72 | 647 | 71 | 4 | 48.8 | 145.5 | 6.2/7.1 | Solodovnikov (1994) |
| 6 | Lena Region tuffs | 70 | 123.5 | 2 (15 mT) | 241 | 245 | 146 | 78 | 40 | 39 | 4 | 49 | 143 | 7.1/7.5 | Kamysheva (1973) |
| 7 | Irkutk ores | 56 | 102 | | 241 | 245 | 292 | −83 | 28 | 6 | 13 | 49 | 122 | 24.9/25.4 | Kravchinsky (1979) |
| 8 | Sytykan and Aikhal sills | 66 | 111.8 | 3 (T) | 241 | 245 | 92.7 | 74.9 | 22 | 56.2 | 4 | 52.6 | 163.2 | 6.6/7.3 | Zhitkov *et al.* (1994) |
| 9 | Siberian Traps | 72 | 114 | 2 (8 mT) | 243 | 245 | 300 | −71 | 18 | 34 | 6 | 44 | 157 | 9.1/10.5 | Kamysheva (1973) |
| 10 | Lena River sediments | 72.6 | 124.7 | 2 (500 °C, 50 mT) | 245 | 256 | 164 | 75 | 131 | 43 | 19 | 45 | 136 | 32/35 | Pisarevsky (1982) |
| 11 | Upper Vilyui intrusives | 65.6 | 108.2 | 2 (A) | 208 | 290 | 81 | 75 | 198 | 143 | 4 | 56 | 168 | 6.7/7.3 | Kamysheva (1971) |
| 12 | Upper Markha region intrusives | 65.6 | 111.7 | 2 (A) | 208 | 290 | 102 | 72 | 71 | 67 | 9 | 46 | 164 | 14/15.9 | Kamysheva (1971) |
| 13 | Mid Vilyui region intrusives | 63 | 112 | 2 (8–15 mT) | 208 | 290 | 117 | 80 | 71 | 146 | 3 | 52 | 140 | 5.5/5.7 | Kamysheva (1971) |
| 14 | Olenek Region intrusions | 70.4 | 120.7 | 2 (10.5 mT) | 208 | 290 | 148 | 72 | 69 | 200 | 9 | 39 | 143 | 13/15 | Kamysheva (1975) |
| 15 | Udzha River intrusions | 71.5 | 116 | 2 (TA) | 208 | 290 | 271 | −71 | 9 | 59 | 6 | 51 | 179 | 9.1/10.5 | Rodionov (1984) |
| 16 | Ygyattin region intrusives | 63.7 | 115.4 | 2 (A) | 241 | 290 | 292 | −84 | 196 | 57 | 7 | 58 | 137 | 14/14 | Kamysheva (1975) |
| 17 | Tungus Syncline intrusives | 68 | 89 | 2 (TA) | 241 | 290 | 95 | 62 | 86 | 7 | 6 | 38 | 157 | 7.2/9.3 | Goncharov (1973) |
| 18 | Ygyattin region intrusives | 64.1 | 114.7 | 2 (A) | 241 | 290 | 114 | 80 | 250 | 50 | 7 | 52 | 144 | 14/14 | Kamysheva (1975) |
| 19 | Morcoca River Intrusives | 65.6 | 110.5 | 2 (A) | 241 | 290 | 83 | 79 | 132 | 100 | 8 | 61 | 157 | 14/15 | Kamysheva (1975) |
| 20 | Markha region volcanics and intrusions combined locality 1 | 66.1 | 111.6 | 2 (A) | 241 | 290 | 136 | 76 | | 300 | 4 | 44 | 137 | 7/7 | Kamysheva (1975) |
| 21 | Markha region volcanics and intrusions combined locality 2 | 66.1 | 111.6 | 2 (A) | 241 | 290 | 261 | −71 | | 87 | 6 | 52 | 177 | 9/10 | Kamysheva (1975) |
| 22 | Klintaiga Group (seds., tuffs, clays) | 58.5 | 102.5 | 2 (A) | 256 | 290 | 100 | 84 | 39 | 17 | 6 | 56 | 122 | 11.6/11.8 | Davydov & Kravchinsky (1971) |
| 23 | Besukea River Redbeds | 69.8 | 128.5 | 2 (ATV) | 256 | 290 | 302 | −45 | 23 | 6 | 13 | 15 | 180 | 10/16 | Pisarevsky & Archegov (1982)) |

Same abbreviations as Table 17.

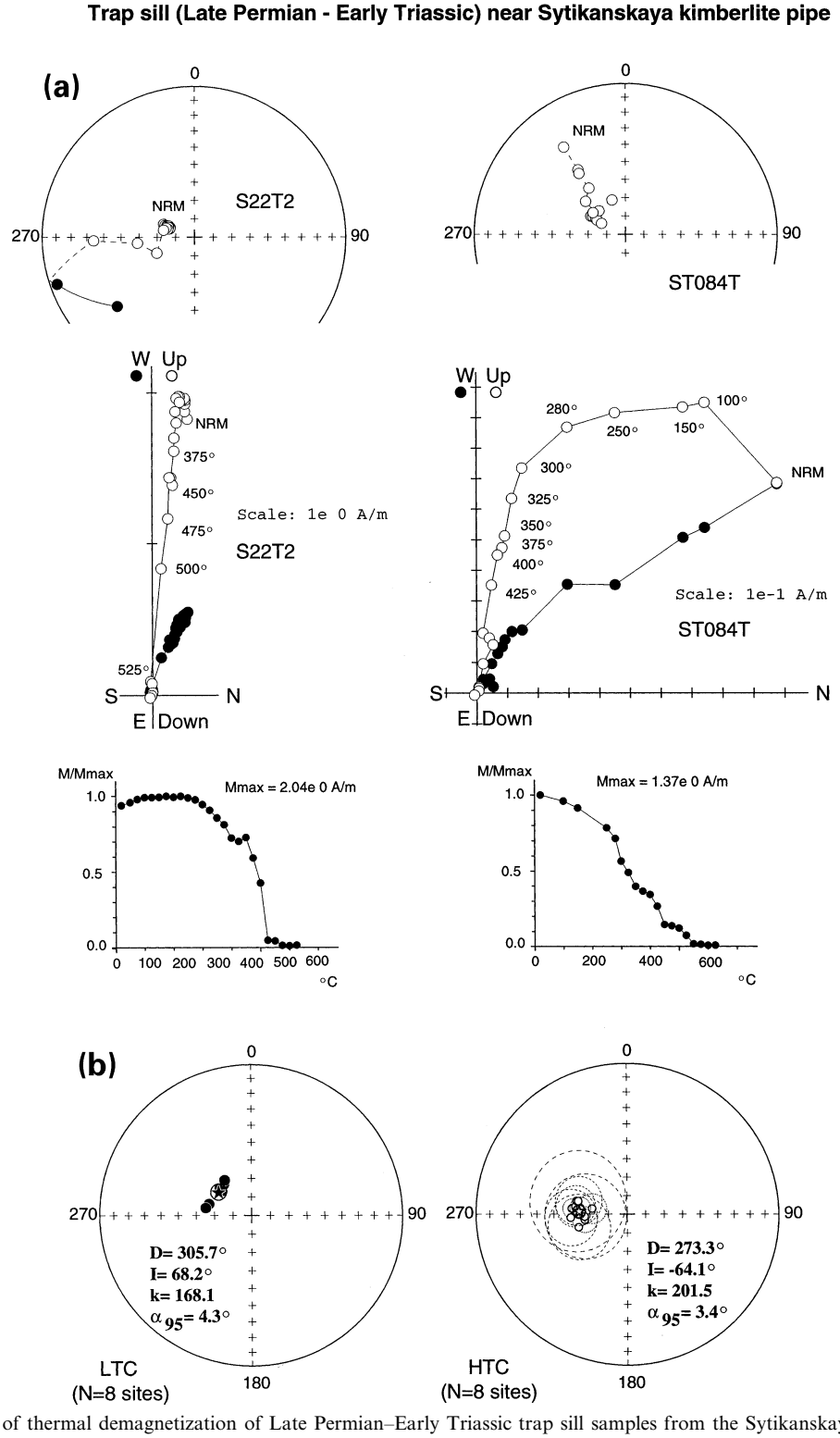


**Figure 15.** (a) Results of thermal demagnetization of Late Permian–Early Triassic trap sill samples from the Sytikanskaya kimberlite pipe area. (b) Equal-area projections of site-mean directions of LTC and HTC, with circles of 95 per cent confidence shown *in situ*.

migrated northwards. Montero *et al.* (2000) showed that closing of the Ural ocean took place between 320 and 255 Ma. The proximity of Siberia to Russia and Kazakhstan at 360 Ma is in agreement with geological data (Zonenshain *et al.* 1990; Nikishin *et al.* 1996). Geological events (subduction complex, granite–gneissic domes under the volcanic arc, folding and metamorphism) during the Late Devonian–Early Tournaisian were connected to the Russia/Kazakhstan collision in the southern Urals and to the Russia/Siberia collision in the northern Urals.

At 250 Ma, Siberia continued its clockwise rotation at high northern latitudes (Fig. 20). The last stage of formation of Northern Eurasia involved final accretion of Russia and Siberia along the Uralian belt. North Eurasia was incorporated

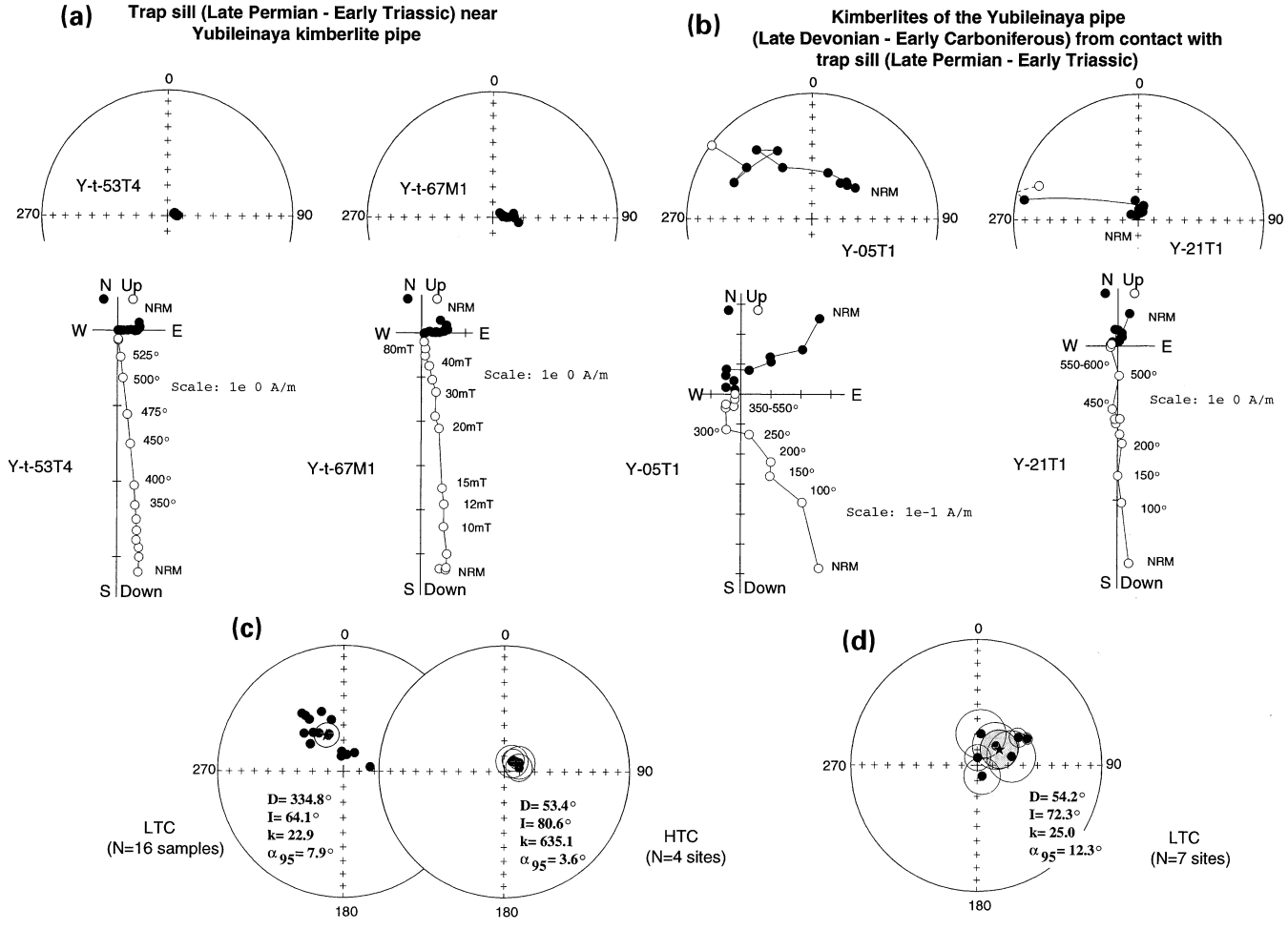


**Figure 16.** Results of thermal and AF demagnetization of Late Permian–Early Triassic trap sill samples from the Yubileinaya kimberlite pipe area (a), and kimberlite samples from the contact with the trap sill zone (baked test) (b). Equal-area projections of site-mean directions of LTC and HTC, with circles of 95 per cent confidence for the Late Permian–Early Triassic trap sill of the Yubileinaya kimberlite pipe area (c), and LTC of kimberlites near contact with the trap sill (baked test) (d). All shown *in situ*. Other details as in Fig. 4.

into Pangaea at this time (Van der Voo 1993; Smethurst *et al.* 1998). We suggest that, as has been found to be the case for many traps (e.g. Courtillot 1994; Courtillot *et al.* 1999), and particularly for the Permo-Triassic Siberian traps (Renne & Basu 1991; Campbell *et al.* 1992; Renne *et al.* 1995; Venkatesan *et al.* 1997; Hofmann 1997), the Late Devonian–Early Carboniferous traps were erupted as a short climactic event. Palaeomagnetic poles are close to each other, and the scatter ($\sigma = 15°$) is typical of secular variation, which is compatible with the idea that all magmatic events were rather close to each other in time. New absolute dating is required to check this hypothesis.

Fig. 20 shows a reconstruction in the Late Devonian, at about 360 Ma. The traps analysed in the present paper and associated with the Viluy rift are shown by light grey shading. The Viluy rift zone itself is evidence of attempted continental break-up and forms one arm of a triple junction feature that we propose, following Zonenshain *et al.* (1990). The missing continental fragment to the north may be the Omolon block (possibly with surrounding microblocks such as Pri-Kolima, Okhotsk, Chersky, etc.). The Omolon block has a pre-Rifean crystalline basement and a sedimentary cover, consisting of sediments and volcanic deposits of Rifean to Early Jurassic age (Terekhov 1979). It is still unclear to which Precambrian platform the Omolon block belonged. Large fold belts surround the block. Even in Mesozoic times, up to the beginning of the Middle Jurassic, the Omolon block was characterized by marine sediments. Accretion with Siberia happened only in the Late Jurassic–Early Cretaceous (Savostin *et al.* 1993). The interpretation of Zonenshain *et al.* (1990) supports our hypothesis. These authors showed that a spreading zone indeed existed between NE of Siberia (along the Verkhoyansk folded zone) and the Chersky block. Available palaeomagnetic data show that both the Omolon and Okhotsk blocks had palaeolatitudes of about 15–30°N in the Late Devonian, close to the palaeolatitude of Siberia. However, geological evidence suggests marine sediments up to the Late Jurassic–Early Cretaceous, when these blocks accreted to Siberia (again?). The concept of a triple junction rift zone is supported by geological arguments (Shpount & Oleinikov 1987). We propose that the active arms of this junction zone were located in the Verkhoyansk folded zone (in present-day coordinates) and to the north of the Siberian platform (dashed line in Fig. 20). It is unclear where the arm of the junction zone that heads towards Lake Baikal stops to the southwest (in present-day coordinates), either at the present southern end of the Viluy aulacogen or further south. Traps are well known north of the Baikal–Patom folded zone, but there is a lack of absolute

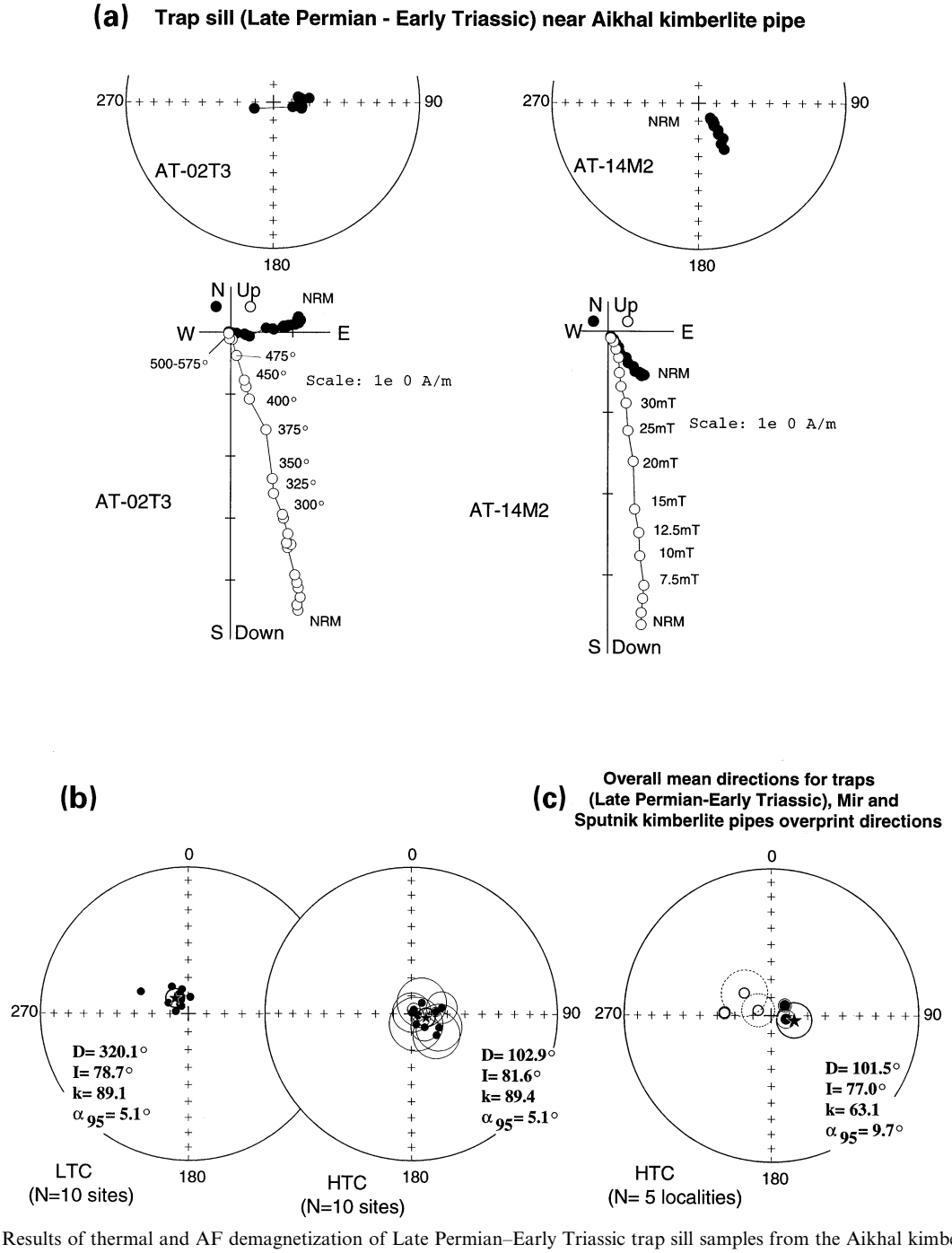


**Figure 17.** (a) Results of thermal and AF demagnetization of Late Permian–Early Triassic trap sill samples from the Aikhal kimberlite pipe area. See Fig. 4 legend for further details. Equal-area projections of site-mean directions of LTC and HTC, with circles 95 per cent of confidence shown in *in situ* coordinates. (b) LTC and HTC for the Late Permian–Early Triassic trap sill of the Aikhal kimberlite pipe area. (c) HTC for all Late Permian–Early Triassic trap sills (area of Sytikanskaya, Yubileinaya and Aikhal kimberlite pipes) and overprint directions of Mir and Sputnik kimberlite pipes. Other details as in Fig. 4.

dating in that region. Some authors consider that basaltic sills and dykes of the Baikal–Patom zone may be Precambrian (Shpount & Oleinikov 1987); others consider that they might be Palaeozoic as in the Viluy region (Masaitis *et al.* 1975).

Several other large trap occurrences are now known near the time of the Devonian–Carboniferous boundary. Volcanic activity was accompanied by rifting and kimberlite magmatism in the Pripyat–Dniepr–Donets aulacogen. Two-thirds of the rifting in this area of the Russian platform occurred rapidly between 367 and 364 Ma (Kusznir *et al.* 1996; Wilson & Lyashkevich 1996). New $^{40}Ar/^{39}Ar$ dating shows that the peak age of Kolva rift magmatism in the Timan–Pechora basin is also close to the Devonian–Carboniferous boundary ($351 \pm 2$ Ma) (Wilson *et al.* 1999). An extensional tectonic regime prevailed in the northern part of the Russian platform during the Devonian. There are formations of this age in the Pechora basin and tectonic grabens in Novaya Zemlya, the Kola Peninsula and possibly the eastern Barents Sea (Gudlaugsson

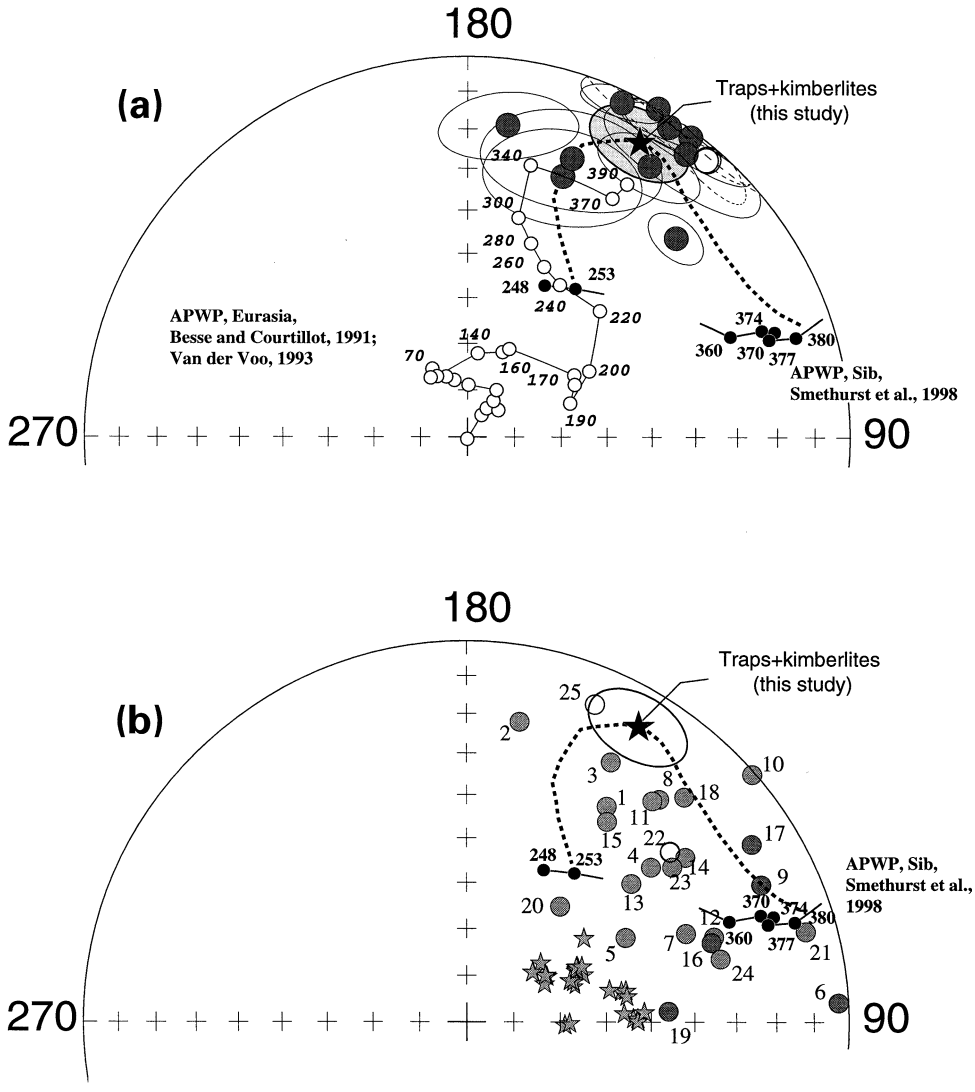


**Figure 18.** (a) Equal-area projection of Late Devonian–Early Carboniferous palaeomagnetic poles from kimberlite pipes and traps obtained in the present study (from Table 16) with their 95 per cent confidence ellipses. Small black dots are the Siberia platform APWP from Smethurst *et al.* (1998) and open circles those from Besse & Courtillot (1991) and Van der Voo (1993), with ages indicated in Myr. Star: mean pole calculated for 11 localities (with its 95 per cent confidence ellipses). Dashed line: proposed Siberian APWP for time interval 380–250 Ma. (b) Equal-area projection of Late Devonian–Early Carboniferous palaeomagnetic poles from the Siberian platform. Poles are taken from the palaeomagnetic database (McElhinny & Lock 1996). Black dots are the Siberia platform APWP for the Palaeozoic (248–538 Ma) from Smethurst *et al.* (1998), with ages indicated in Myr. The numbers close to the poles correspond to the numbers in Table 17. Grey stars show sampling localities.

*et al.* 1998). Voluminous alkaline magmatism occurred in the Kola Peninsula from 380 to 360 Ma, coinciding with the subsidence of the NE–SW-trending Kontozero graben (Kramm *et al.* 1993), and contemporaneous with Late Frasnian–Famennian (370–363 Ma) alkaline magmatism in the Dnieper–Donets rift on the southern margin of the Russian platform (Wilson & Lyashkevich 1996). Our palaeomagnetic results lead us to propose that trap magmatism may also have been quite fast in the Viluy rift system. Clearly, the end of the Devonian was a time of extremely widespread trap magmatism and rifting in many of the blocks that were to form Eurasia, especially the Russian and Siberian platforms. Sedimentary constraints on the age of rifting and available geochronological data (unfortunately still too few, and often uncertain or obsolete) appear to be compatible with the idea that much of the magmatism was short-lived and coeval, near or at the time of the Frasnian–Famennian boundary. This is the time of the largest mass-extinction event before the end of the Palaeozoic (Sepkoski 1990; Gregorz 1998). This would complement the sequence of trap/extinction (plus rifting) episodes that punctuated much of the Phanerozoic (Courtillot 1994; Courtillot *et al.* 1999). The Russia–Siberian trap province would appear to be one of the largest trap events (despite the scarcity of remnants), similar to the Central Atlantic Magmatic Province (CAMP) province at 200 Ma, which is gradually emerging as one of the largest trap events (at least with the largest surface extent) (Olsen 1999; Marzoli *et al.* 1999).

In our 250 Ma reconstruction (Fig. 20), the Permo-Triassic traps in Siberia have been emphasized in light grey shading. Three possible areas of a triple junction break-up are very tentatively indicated as thick dashed lines. There is no clear evidence for rifting between Siberia and Kazakhstan following the trap event and many authors consider that indeed there was no break-up following magmatism. Nesterov *et al.* (1995) write

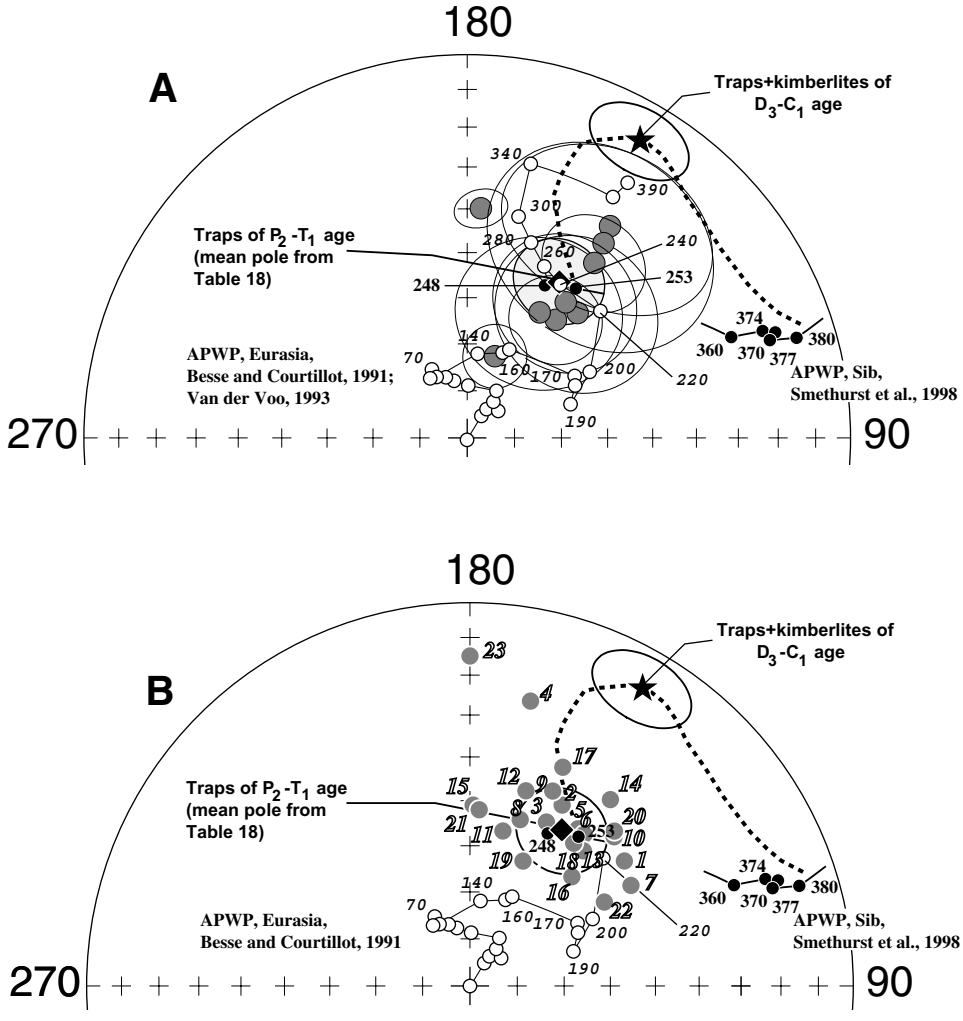


**Figure 19.** (a) Equal-area projection of Late Permian–Early Triassic palaeomagnetic poles from the Siberian traps obtained in the present study (from Table 18) with their 95 per cent confidence ellipses. Diamond: mean pole calculated for nine localities (with its 95 per cent confidence ellipses). (b) Equal-area projection of Late Permian–Early Triassic palaeomagnetic poles from the Siberian platform. Poles are taken from the palaeomagnetic database (McElhinny & Lock 1996). Numbers near poles corresponds to numbers in Table 19. Other details as in Fig. 18.

that continental 'lake and plain' landscapes were dominant. No marine foraminifera have been found, although analysis of mudstones from boreholes suggests that the area was flooded at times by the sea. However, some authors suggested the existence of the so-called Ob palaeo-ocean (Aplonov 1987) further north. Zonenshain *et al*. (1990) describe Triassic rifting, which affected the Barents Sea basin, when intraplate magmatism continued to be extensive and flood basalts covered vast areas of North Siberia. This might be a later stage linked to rifting. Almukhamedov *et al*. (1996) showed that a rifting stage of magmatism indeed characterizes traps in the Western Siberian basin. At the same time the middle and late stages of Western Siberian trap magmatism are low-K and may not characterize rift magmatism.

Occurrences of basalt magmatism over most of the northern part of the platform (north of the Anabar shield; see Fig. 2), witnessed from drilling data in Western Siberia, lead us to propose a tentative triple junction outline, in which one arm attempts to split the Siberian continent (Fig. 20), a second arm follows the Anabar shield at constant latitude, and a third enters the Arctic ocean (all in present-day coordinates). Taimyr and Severnaya Zemlya, north of the Siberian platform, consist of three different zones: Northern, Central and Southern Taimyr (Zonenshain *et al*. 1990). Only the southern block (the Southern Taimyr zone) belongs to the Siberian passive margin. The other two are geologically significantly different from Siberia. Northern Taimyr (part of Laurussia) collided with Central Taimyr at the end of the Palaeozoic. The meaning and position of the Central Taimyr zone is still uncertain. We propose that one of the arms of the triple junction rift zone followed the South Taimyr fold belt, which is directed ENE. Clearly, this hypothetical model needs further work.

As far as the apparent polar wander path of Siberia is concerned, the most recent review was proposed by Smethurst *et al*. (1998). These authors believed that data were sufficient to propose a tentative APWP between 380 and 360 Ma, but considered that there were no reliable data between 360 and 250 Ma, that is, the time of Siberian trap volcanism, which marked the onset of a reasonably well-constrained APWP. We have been able to propose a new reliable pole at 360 Ma, which is remote from the Smethurst *et al*. (1998) segment, generating a very large loop in the Siberian APWP (shown in Figs 18 and 19

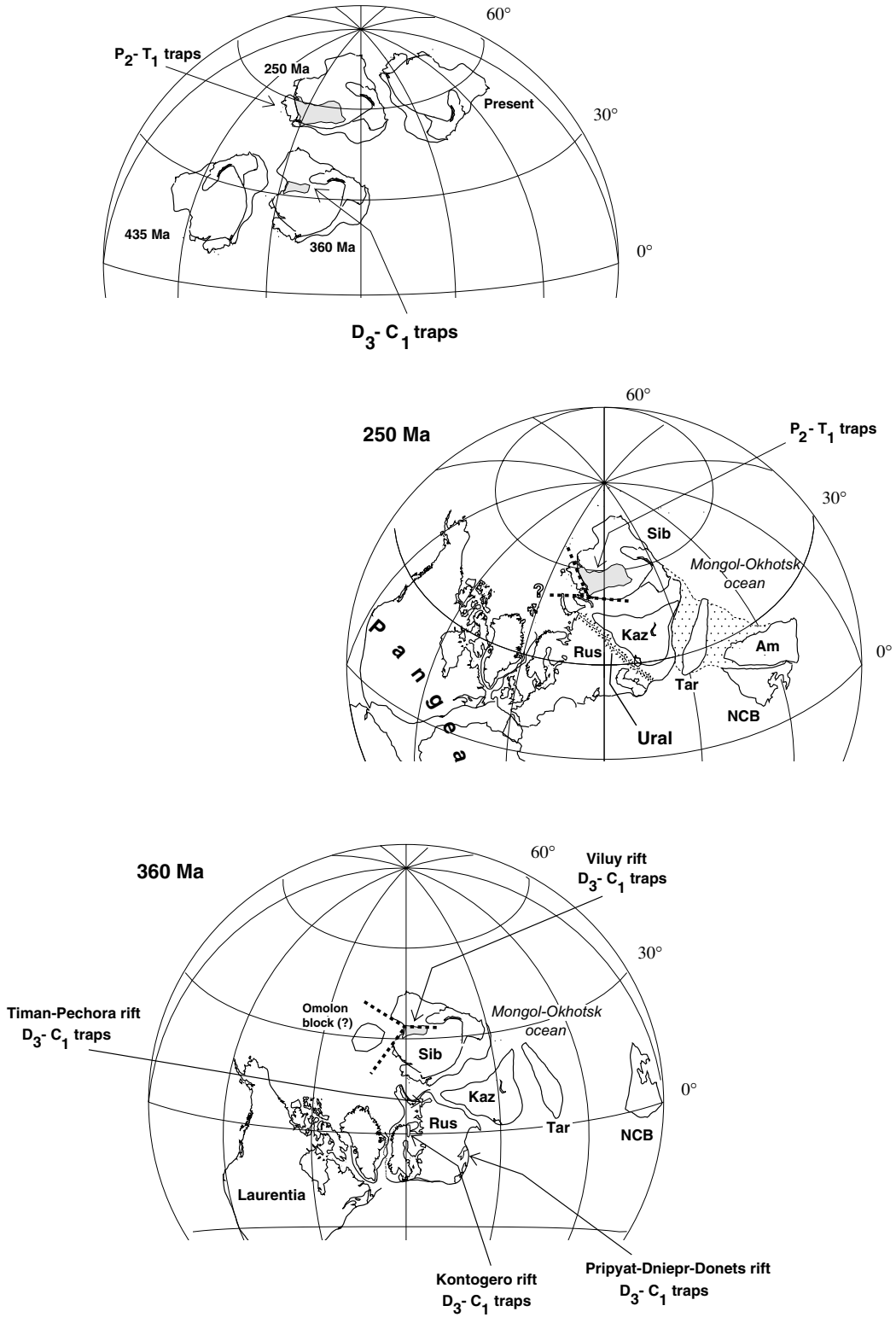


**Figure 20.** Palaeogeographic reconstructions of the Siberian platform and surrounding blocks at 250 Ma (centre) and 360 (bottom), and overall motion of Siberia from 435 Ma to present (top). Block limits and features within the Siberian craton from Fig. 1. Possible rifts (shaded areas) and triple junctions (dashed lines) associated with the Late Devonian and Early Triassic traps are shown. Also shown in the bottom (360 Ma) reconstruction are widespread occurrences of coeval traps and rifts on the Russian platform (see text).

by a dashed line). Fast polar wander is implied in the few tens of millions of years preceding the large 360 Ma (Frasnian–Famennian (?)) trap event, and a large gap remains between the two trap poles proposed in this paper, that is, over an interval of 110 Myr. Therefore, additional palaeomagnetic and geochronological work is still required before more accurate paths, and resulting palaeogeographic reconstructions, can be obtained. However, the close proximity of the Siberian, Russian

and Kazakhstan platforms as early as 360 Ma suggests that rearrangements occurred and that the overall configuration of much of what was to become Eurasia remained relatively stable over time.

## ACKNOWLEDGMENTS

We express our deep gratitude for assistance in conducting the work and/or valuable advice from A. I. Almukhamedov, J. Besse, S. M. Bezborodov, J.-P. Cogné, S. Gilder, M. Z. Khuzin, L. P. Koukhar, M. A. Krainov, E. A. Kravchuk, M. I. Kuzmin, A. Ya. Medvedev, N. Peterson, N. A. Sadovnikova and A. S. Zasypkin. We thank A. N. Zhitkov, who initiated this work and took part in the beginning of the study, and J.-P. Cogné and R. Enkin for free use of their computer program packages. We thank R. Van der Voo and an anonymous reviewer as well as C. G. Langereis for their helpful comments and suggestions. This research was funded by the Botuobinskaya Geological Company, Amakinskaya Geological Company and Institut de Physique du Globe de Paris. This is contribution 1761 of the Institut de Physique du Globe de Paris.

## REFERENCES

Almukhamedov, A.I. & Zolotukhin, V.V., 1989. Geochemical stratigraphy of basalts of North-West of Siberian platform, *Doklady Acad. Sci. USSR,* **306,** 963–967 (in Russian).

Almukhamedov, A.I., Medvedev, A.Ya, Mitchell, C. & Zolotukhin, V.V., 1996. Flood basalts in the core of the Tunguska syneclinse: comparative geochemistry, *Russian Geol. Geophys., Novosibirsk,* **37,** 3–16 (in Russian).

Aparin, V.P., 1973. Paleomagnetic pole, in Paleomagnetic directions and pole positions: Data for the USSR, *Catalogue Issue 2,* Soviet Geophysical Committee: World Data Center-B (Moscow).

Aplonov, S.V., 1987. *Geodynamics of the Early Mesozoic Ob Paleoocean, Nauka Press*, Leningrad (in Russian).

Bai, Y., Chen, G., Sun, Q., Sun, Y., Li, Y., Dong, Y. & Sun, D., 1987. Late Paleozoic polar wander path for the Tarim platform and its tectonic significance, *Tectonophysics,* **139,** 145–153.

Besse, J. & Courtillot, V., 1991. Revised and synthetic apparent polar wander paths of African, Eurasian, North-American and Indian true polar wander since 200 Ma, *J. geophys. Res.,* **96,** 4029–4050.

Brakhfogel, F.F., 1984. *Geological Aspects of Kimberlite Magmatism in the Northeastern Siberian Platform,* Publ. Yakutian Institute of Geology, Russian Academy of Sciences, Yakutsk (in Russian).

Campbell, I.H., Czmanske, G.K. & Fedorenko, V.A., Hill, R.I. & Stepanov, V., 1992. Synchronism of the Siberian traps and the Permian–Triassic boundary, *Science,* **258,** 1760–1763.

Cogné, J.P., 2000. *A Macintosh Application for Paleomagnetic Data Processing and Plate Reconstructions (PaleoMac 4),* Institut de Physique du Globe de Paris, University de Paris 7, Paris.

Courtillot, V., 1994. Mass extintions in the last 300 million years: one impact and seven flood basalts?, *Isr. J. Earth Sci.,* **43,** 255–266.

Courtillot, V., Jaupart, C., Manighetti, I., Tapponnier, P. & Besse, J., 1999. On causal links between flood basalts and continental breakup, *Earth planet. Sci. Lett.,* **166,** 177–195.

Dalziel, I.W.D., Lawver, L.A. & Murphy, J.B., 2000. Plumes, orogenesis, and supercontinental fragmentation, *Earth planet. Sci. Lett.,* **178,** 1–11.

Davydov, V.F. & Kravchinsky, A.Y., 1971. Paleomagnetic pole, in Paleomagnetic directions and pole positions: data for the USSR, *Catalogue Issue 1,* Soviet Geophysical Committee, World Data Center-B, Moscow.

Davydov, V.F. & Kravchinsky, A.Y., 1973. Paleomagnetic pole, in Paleomagnetic directions and pole positions: data for the USSR, *Catalogue Issue 2,* Soviet Geophysical Committee, World Data Center-B, Moscow.

Dunlop, D.J. & Ozdemir, O., 1997. Rock Magnetism, *Fundamentals and Frontiers,* Cambridge University Press, Cambridge.

Enkin, R.J., 1996. *A Computer Program Package for Analysis and Presentation of Paleomagnetic Data,* Pacific Geoscience Center, Geological Survey of Canada, Victoria.

Enkin, R.J., Yang, Z., Chen, Y. & Courtillot, V., 1992. Paleomagnetic constraints on the geodynamic history of the major blocks of China from the Permian to the Present, *J. geophys. Res.,* **97,** 13 953–13 989.

Fisher, R., 1953. Dispersion on a sphere, *Proc. R. Soc. Lond., Series,* **A217,** 295–305.

Gilder, S. & Courtillot, V., 1997. Timing of the North-South China collision from new middle to late Mesozoic paleomagnetic data from the North China Block, *J. geophys. Res.,* **102,** 17 713–17 727.

Gilder, S., Zhao, X., Coe, R., Meng, Z., Courtillot, V. & Besse, J., 1996. Paleomagnetism and tectonics of the southern Tarim basin, northwestern China, *J. geophys. Res.,* **101,** 22 015–22 031.

Goncharov, G.I., 1973, Paleomagnetic pole, in Paleomagnetic directions and pole positions: Data for the USSR, *Catalogue Issue 2,* Soviet Geophysical Committee: World Data Center-B (Moscow).

Griffin, W.L. *et al.*, 1999. The Siberian lithosphere traverse, mantle terranes and the assembly of the Siberian Craton, *Tectonophysics,* **310,** 1–35.

Grzegorz, R., 1998. Frasnian-Famennian biotic crisis: undervalued tectonic control?, *Paleogeogr., Paleoclimat., Paleoecol.,* **141,** 177–198.

Gudlaugsson, S.T., Faleide, J.I., Johansen, S.E. & Breivik, A.J., 1998. Late Palaeozoic structural development of the south-western Barents Sea, *Mar. Petrol. Geol.,* **15,** 73–102.

Gurevitch, E., Westphal, M., Daragan-Suchov, J., Fainberg, H., Pozzi, J.P. & Khramov, A.N., 1995. Paleomagnetism and magnetostratigraphy of the traps from Western Taimir (northern Siberia) and the Permo-Triassic crisis, *Earth planet. Sci. Lett.,* **136,** 461–473.

Gusev, G.S. & Khain, V.E., 1995. On the relationship of Baikal-Patom, Aldan-Vitim and Mongol-Okhotsk terrains (south of Middle Siberia), *Geotektonika, Moscow,* **5,** 68–82 (in Russian).

Halim, N., Kravchinsky, V., Gilder, S., Cogné, J.-P., Alexutin, M., Sorokin, A., Courtillot, V. & Chen, Y., 1998. A palaeomagnetic study from the Mongol-Okhotsk region, rotated Early Cretaceous volcanics and remagnetized Mesozoic sediments, *Earth planet. Sci. Lett.,* **159,** 133–145.

Halls, H.C., 1976. A least-squares method to find a remanence direction from converging remagnetization circles, *Geophys. J. R. astr. Soc.,* **45,** 297–304.

Hofmann, C., 1997. Datation $^{40}Ar/^{39}Ar$ et paléomagnétisme des traps d'Ethiopie, du Deccan et de Sibérie, *PhD thesis,* University of Paris 7 and Institut de Physique du Globe de Paris, Paris, France.

Kamysheva, G.G., 1971. Paleomagnetic pole, in Paleomagnetic directions and pole positions: Data for the USSR, *Catalogue Issue 1,* Soviet Geophysical Committee: World Data Center-B (Moscow).

Kamysheva, G.G., 1973. Paleomagnetic pole, in Paleomagnetic directions and pole positions: Data for the USSR, *Catalogue Issue 2,* Soviet Geophysical Committee, World Data Center-B, Moscow.

Kamysheva, G.G., 1975. Paleomagnetic pole, in Paleomagnetic directions and pole positions: Data for the USSR, *Catalogue Issue 2,* Soviet Geophysical Committee, World Data Center-B, Moscow.

Kirschvink, J.L., 1980. The least-squares line and plane and the analysis of paleomagnetic data, *Geophys. J. R. astr. Soc.,* **62,** 699–718.

Kramm, U., Kogarko, L.N., Kononova, V.A. & Vartiainen, H., 1993. The Kola alkaline province of the CIS and Finland: precise Rb–Sr ages define 380–360 Ma age range for all magmatism, *Lithos,* **30,** 33–44.

Kravchinsky, A.Ya., 1979. *Paleomagnetism and Paleogeographic Evolution of Continents,* Nauka, Novosibirsk (in Russian).

Kravchinsky, V.A., 1990. Horizontal movements of tectonic blocks of the Mongol-Okhotsk geosuture, in *Present Geophysical Investigations of the Eastern Siberia,* pp. 102–105, ed. Mukhalevsky, V.I., Eastern Siberian Pravda, Irkutsk (in Russian).

Kravchinsky, V.A., Cogné, J.-P., Harbert, W. & Kuzmin, M.I., 2002. Evolution of the Mongol-Okhotsk ocean with paleomagnetic data from the suture zone, *Geophys. J. Int.,* in press.

Krivonos, V.F., 1997. Relative and absolute age of kimberlites, *Otechestvennaya Geologiya,* **1,** 41–51 (in Russian).

Kuzmin, M.I., Fillipova, I.B., 1979. The history of the Mongol-Okhotsk belt in the Middle-Late Palaeozoic and Mesozoic, in *Lithospheric Plate Structure,* edited by Zonenshain, L.P., Institute of Oceanology, USSR Academic Science, Moscow, pp. 189–226 (in Russian).

Kusznir, N.J., Kokhuto, A. & Stephenson, R.A., 1996. Synrift evolution of the Pripyat Trough: constraints from structural and stratigraphic modeling, *Tectonophysics,* **268,** 221–236.

Li, Y. *et al.*, 1990. Devonian paleomagnetic pole from red beds of the Tarim Block, China, *J. geophys. Res.,* **95,** 19 185–19 198.

Li, Z.X., Powell, C.McA. & Trench, A., 1993. Palaeozoic global reconstructions, in *Palaeozoic Vertevrate Biostratigraphy and Biogeography,* pp. 25–53, ed. Long, J.A., Belhaven Press, London.

Lind, E.N., 1973. Paleomagnetic pole, in Paleomagnetic directions and pole positions: Data for the USSR, *Catalogue Issue 2,* Soviet Geophysical Committee: World Data Center-B (Moscow).

Lind, E.N., Kropotov, S.V., Czamanske, G.K., Gromme, S.C. & Fedorenko, V.A., 1994. Paleomagnetism of the Siberian flood basalts of the Noril'sk area: a constraint on eruption duration, *Int. geol. Rev.,* **36,** 1139–1150.

Lozhkina, N.V., 1981. Remanent magnetization of Middle-Upper Triassic rocks of the Omolon massif, in *Rock Magnetism and Paleomagnetic Stratigraphy of Eastern and Northern Asia,* pp. 97–106, ed. Lin'kova, T.I., Far East Branch of Russian Academy of Science, Magadan (in Russian).

Marshall, M. & Cox, A., 1971. Effects of oxidation on the natural remanent magnetization of titanomagnetite in sub-oceanic basalts, *Nature,* **230,** 28–31.

Marzoli, A., Renne, P.R., Piccirillo, E.M., Ernesto, M., Bellieni, G. & De Min, A., 1999. Extensive 200 million-years-old continental flood basalts of the Central Atlantic Magnetic Province, *Science,* **284,** 616–618.

Masaitis, V.L., Mikhailov, M.V. & Selivanovskaya, T.B., 1975. *Volcanism and Tectonics of the Patom-Viluy Middle Paleozoic Aulacogen,* Nedra, Moscow (in Russian).

McElhinny, M.W., 1964. Statistical significance of the fold test in paleomagnetism, *Geophys. J. R. astr. Soc.,* **8,** 338–340.

McElhinny, M.W. & Lock, J., 1996. IAGA paleomagnetic databases with access, *Surv. Geophys.,* **17,** 575–591.

McFadden, P.L. & Lowes, F.J., 1981. The discrimination of mean directions drawn from Fisher distributions, *Geophys. J. R. astr. Soc.,* **67,** 19–33.

McFadden, P.L. & McElhinny, M.W., 1988. The combined analysis of remagnetization and direct observation in paleomagnetism, *Earth planet. Sci. Lett.,* **87,** 161–172.

Montero, P., Bea, F., Gerdes, A., Fershtater, G., Zin'kova, E., Borodina, N., Osipova, T. & Smirnov, V., 2000. Single-zircon evaporation ages and Rb–Sr dating of four major Variscan batholiths of the Urals: a perspective on the timing of deformation and granite generation, *Tectonophysics,* **317,** 93–108.

Nesterov, I.I., Bochkarev, V.S. & Purtova, S.T., 1995. A unique section of Triassic sediments in West Siberia, *Doklady Akademii Nauk, Ser. Geol.,* **340,** 659–663 (in Russian).

Nikishin, A.M. *et al.*, 1996. Late Precambrian to Triassic history of the East-European Craton: dynamics of sedimentary basin evolution, *Tectonophysics,* **268,** 23–63.

Oleinikov, B.V., 1979. *Geocemistry and Orogenesis Continental Flood Basalts,* Nauka, Novosibirsk (in Russian).

Olsen, P.E., 1999. Giant lava flows, mass extinctions, and mantle plumes, *Science,* **284,** 604–605.

Parfenov, L.M., 1984. *Continental Margins and Island Arcs of Mesozoids of North-Western Asia,* Nauka, Novosibirsk (in Russian).

Pechersky, D.M. & Didenko, A.N., 1995. *Paleozoic Ocean, Petromagnetic and Paleomagnetic Information of the Lithosphere,* OEFZ RAN, Moscow (in Russian).

Pisarevsky, S.A., 1982. Paleomagnetic pole, in Paleomagnetic directions and pole positions: Data for the USSR, *Catalogue Issue 5,* Soviet Geophysical Committee, World Data Center-B, Moscow.

Pisarevsky, S.A., & Archegov, V.B. 1982. Paleomagnetic pole, in Paleomagnetic directions and pole positions: Data for the USSR, *Catalogue Issue 5,* Soviet Geophysical Committee: World Data, Center-B (Moscow).

Renne, P. & Basu, A.R., 1991. Rapid eruption of the Siberian traps flood basalts at the Permo–Triassic boundary, *Science,* **253,** 176–179.

Renne, P., Zichao, Z., Richards, M.A., Black, M.T. & Basu, A., 1995. Synchrony and causal relations between Permian–Triassic boundary crises and Siberian flood volcanism, *Science,* **269,** 1413–1415.

Rodionov, V.P., 1984. Palaeomagnetism of Upper Precambrian and Lower Palaeozoic of the Udzha River region, in *Palaeomagnetic Methods for Stratigraphy,* pp. 18–29, ed. Khramov, A.N., VNIGRI Publishing, Leningrad (in Russian).

Rodionov, V.P. & Komissarova, R.A., 1975. Paleomagnetic pole, in Paleomagnetic directions and pole positions: Data for the USSR, *Catalogue Issue 3,* Soviet Geophysical Committee: World Data Center-B (Moscow).

Rosen, O.M., Condie, K.C., Natapov, L.M. & Nozhkin, A.D., 1994. Archean and Early Proterozoic evolution of the Siberian craton: a preliminary assessment, in *Archean Crustal Evolution*, pp. 411–459, ed. Condie, K.C., Elsevier, Amsterdam.

Savostin, L.A., Pavlov, V.E., Safonov, V.G. & Bondarenko, G.E., 1993. Lower and middle Jurassic deposits in the Western Zone of the Omolon Block (Northeastern Russia): conditions of formation and paleomagnetism, *Doklady Akademii Nauk SSSR,* **333,** 481–486 (in Russian).

Savrasov, J.I. & Kamisheva, G.G., 1963. Directions of natural remanent magnetization in kimberlites, in *Issue V Paleomagnetic Conference,* PP. 124–129, Siberian Branch of Russian Academy of Science, Krasnoyarsk (in Russian).

Sepkoski, J.J., Jr, 1990. The taxonomic structure of periodic extinction, in *Global Catastrophes in Earth History: An Interdisciplinary Conference on Impacts, Volcanism, and Mass Mortality,* eds Sharpton, V.L. & Ward, P.D., *Geol. Soc. Am. Spec. Pap.,* **247,** 33–44.

Shpount, B.R. & Oleinikov, B.V., 1987. A comparison of mafic dike swarms from the Siberian and Russian platforms, in *Mafic Dyke Swams*, pp. 379–384, eds Halls, H.C. & Fahrig, W.F., Geological Assoc. of Canada, St. Johns.

Smethurst, M.A. & Khramov, A.N., 1992. A new Devonian palaeomagnetic pole for the Russian platform and Baltica, and related apparent polar wander, *Geophys. J. Int.,* **108,** 179–192.

Smethurst, M.A., Khramov, A.N. & Torsvik, T.H., 1998. The Neoproterozoic and Palaeozoic palaeomagnetic data for the Siberian Platform: From Rodinia to Pangea, *Earth Sci. Rev.,* **43,** 1–21.

Solodovnikov, G.M., 1994. Paleointensity of the geomagnetic field in Early Triassic, *Fizika Zemli, Moscow,* **9,** 72–79 (in Russian).

Surkov, V.S., Devyatov, V.P., Zhero, O.G., Kazakov, A.M., Kramnik, V.N. & Smirnov, L.V., 1993. Structure of the Earth's crust in the Tyumen superseep borehole zone, *Russian Geol. Geophys.,* **34,** 120–126.

Terekhov, M.I., 1979. *Stratigraphy and Tectonics of South Part of the Omolon Block,* Nauka, Moscow.

van der Voo, R., 1993. *Paleomagnetism of the Atlantic, Tethys, and Iapetus Oceans,* Cambridge University Press, Cambridge.

Van Fossen, M.C. & Kent, D.V., 1993. A palaeomagnetic study of 143 Ma kimberlite dykes in central New York State, *Geophys. J. Int.,* **113,** 175–185.

Venkatesan, T.R., Kumar, A., Gopalan, K. & Almukhamedov, A.I., 1997. $^{40}$Ar-$^{39}$Ar age of Siberian basaltic volcanism. *Chem. Geol.,* **138,** 303–310.

Vinarsky, Ya.S., Zhitkov, A.N., Kravchinsky, A.Ya., 1987. Automated System OPAL for Processing Palaeomagnetic Data. Algorithms and Programs. VIAMS, Moscow (in Russian).

Watson, G.S. & Enkin, R.J., 1993. The fold test in paleomagnetism as a parameter estimation problem, *Geophys Res. Lett.,* **20,** 2135–2137.

Westphal, M., Gurevitch, E.L., Samsonov, B.V., Feinberg, H. & Pozzi, J.-P., 1998. Magnetostratigraphy of the lower Triassic volcanics from deep drill SG6 in western Siberia: evidence for long-lasting Permo-Triassic volcanic activity, *Geophys. J. Int.,* **134,** 254–266.

Wilson, M. & Lyashkevich, Z.M., 1996. Magmatism and the geodynamics of rifting of the Pripyat-Dnieper rift, East European Platform, *Tectonophysics,* **268,** 64–81.

Wilson, M., Wijbrans, J., Fokin, P.A., Nikishin, A.M., Gorbachev, V.I. & Nazarevich, B.P., 1999. $^{40}Ar/^{39}Ar$ dating, geochemistry and tectonic setting of Early Carboniferous dolerite sills in the Pechora basin, foreland of the Polar Urals, *Tectonophysics,* **313,** 107–118.

Xu, X., Harbert, W., Drill, S. & Kravchinsky, V., 1997. New paleomagnetic data from the Mongol-Okhotsk collision zone, Chita region, south-central Russia, implications for Paleozoic paleogeography of the Mongol-Okhotsk ocean, *Tectonophysics,* **269,** 113–129.

Zhao, X., Coe, R.S., Zhou, Y.X., Wu, H.R. & Wang, J., 1990. New palaeomagnetic results from northern China, collision and suturing with Siberia and Kazakhstan, *Tectonophysics,* **181,** 43–81.

Zhao, X., Coe, R.S., Gilder, S.A. & Frost, G.M., 1996. Paleomagnetic constraints on the palaeogeography of China: implications for Gondwanaland, *Aust. J. Earth Sci.,* **43,** 643–672.

Zhitkov, A.N., Kravchinsky, V.A. & Konstantinov, K.M., 1994. Paleomagnetic studies aimed at obtaining paleomagnetic data for the geodynamics of the eastern USSR (east of the Enisey river), *Rept on Theme 01423412334 for 1991–1994,* Geological Committee of Russia, Irkutsk (in Russian).

Zijderveld, J.D.A., 1967. A.C. demagnetization of rocks, analysis of results, in *Methods in Paleomagnetism*, pp. 254–286, eds Collinson, D.W., Creer, K.M. & Runcorn, S.K., Elsevier, Amsterdam.

Zolotukhin, V.V. & Almukhamedov, A.I., 1988. Traps of Siberian platform, in *Continental Flood Basalts,* pp. 273–310, ed. Macdougall, J.D., Kluver Academic, Dordrech.

Zonenshain, L.P., Kuzmin, M.I. & Natapov, L.M., 1990. *Tectonics of Lithosphere Plates of the Territory of the USSR,* Vol. 1, Nedra, Moscow (in Russian).